Plains CO_2 Reduction (PCOR) Partnership
Energy & Environmental Research Center (EERC)

BELL CREEK TEST SITE – SIMULATION REPORT

Plains CO_2 Reduction (PCOR) Partnership Phase III
Task 9 – Deliverable D66
Update 2

Originally Submitted: August 2011
Update 1 Submitted: August 2012

Prepared for:

William Aljoe

National Energy Technology Laboratory
U.S. Department of Energy
626 Cochrans Mill Road
PO Box 10940
Pittsburgh, PA 15236-0940

DOE Cooperative Agreement No. DE-FC26-05NT42592

The information and results presented within this annually updated report represent work performed by the EERC as part of the PCOR Partnership Program. The content represents the authors' views and interpretations at the time the report was written. However, in keeping with the EERC's adaptive management approach, the geologic model and simulations are iteratively updated as new information becomes available. As a result, future versions of Deliverable D66 may contain new data and interpretations that may supersede the information within this report.

Prepared by:

Charles D. Gorecki
Wesley D. Peck
Scott C. Ayash
John A. Hamling
Edward N. Steadman
John A. Harju
Jason R. Braunberger
Hui Pu
Terry P. Bailey
Jordan M. Bremer
Panqing Gao
Guoxiang Liu

Energy & Environmental Research Center
University of North Dakota
15 North 23rd Street, Stop 9018
Grand Forks, ND 58202-9018

August 2013
Approved

2018-EERC-05-16

EERC DISCLAIMER

LEGAL NOTICE This research report was prepared by the Energy & Environmental Research Center (EERC), an agency of the University of North Dakota, as an account of work sponsored by the U.S. Department of Energy. Because of the research nature of the work performed, neither the EERC nor any of its employees makes any warranty, express or implied, or assumes any legal liability or responsibility for the accuracy, completeness, or usefulness of any information, apparatus, product, or process disclosed or represents that its use would not infringe privately owned rights. Reference herein to any specific commercial product, process, or service by trade name, trademark, manufacturer, or otherwise does not necessarily constitute or imply its endorsement or recommendation by the EERC.

ACKNOWLEDGMENTS

This work was performed under the U.S. Department of Energy (DOE) Cooperative Agreement No. DE-FC26-05NT42592. The EERC would like to thank Denbury Onshore LLC (Denbury) for providing necessary data to perform this work. Special thanks go to the members of Denbury's Bell Creek team for their valuable input and fruitful discussions. The authors acknowledge the members of the EERC's Editing and Graphics staff. The help of Neil W. Dotzenrod and Megan M. Grove with the creation of several new figures for this report is gratefully acknowledged.

DOE DISCLAIMER

This report was prepared as an account of work sponsored by an agency of the United States Government. Neither the United States Government, nor any agency thereof, nor any of their employees, makes any warranty, express or implied, or assumes any legal liability or responsibility for the accuracy, completeness, or usefulness of any information, apparatus, product, or process disclosed, or represents that its use would not infringe privately owned rights. Reference herein to any specific commercial product, process, or service by trade name, trademark, manufacturer, or otherwise does not necessarily constitute or imply its endorsement, recommendation, or favoring by the United States Government or any agency thereof. The views and opinions of authors expressed herein do not necessarily state or reflect those of the United States Government or any agency thereof.

TABLE OF CONTENTS

Continued…

TABLE OF CONTENTS (continued)

LIST OF FIGURES

Continued…

LIST OF FIGURES (continued)

Continued…

LIST OF FIGURES (continued)

LIST OF TABLES

EXECUTIVE SUMMARY

The Plains CO_2 Reduction (PCOR) Partnership is working with Denbury Resources Inc. (Denbury) to evaluate the effectiveness of large-scale injection of carbon dioxide (CO_2) into the Bell Creek oil field for CO_2 enhanced oil recovery (EOR) and to study long-term incidental CO_2 storage. Discovered in 1967, the Bell Creek oil field in southeastern Montana has undergone primary production (solution gas drive), waterflooding, and two micellar–polymer pilot tests. About 37.7% of the estimated 353 million barrels (MMbbl) of original oil in place (OOIP) has been produced to date. It is anticipated that approximately 30 MMbbl of additional oil will be produced through CO_2 EOR in this field.

With the goal of providing a comprehensive assessment of incidental CO_2 storage behavior, members of the PCOR Partnership have initiated a modeling and numerical simulation program to 1) characterize and model the study area using advanced geologic modeling workflows; 2) develop a robust pressure, volume, and temperature (PVT) model to predict miscibility behavior of the CO_2–Bell Creek crude system and to aid in compositional simulation; 3) history-match the constructed dynamic reservoir model, and 4) utilize predictive simulations to aid in monitoring long-term behavior of injected CO_2.

A detailed 3-D static geocellular model of the Bell Creek oil field area (Version 2 model) was constructed utilizing pertinent reservoir characterization data gathered in an extensive literature review and current core analysis work for the entire Bell Creek oil field and surrounding area. Seven hundred forty-eight wells with wireline logs and many with core data were analyzed, interpreted, and incorporated into the 3-D static geocellular and dynamic reservoir models to represent geologic stratigraphy, petrophysical facies, and reservoir properties in order to provide a solid groundwork for simulation activities.

A seven-component Peng–Robinson equation-of-state (EOS) model was developed and tuned to laboratory PVT tests from Bell Creek crude oil samples in Computer Modelling Group's Winprop software package. The EOS was tuned and matched to the original crude oil and yield minimum miscibility pressure (MMP) of 2970 psia, which was close to the experimental MMP estimated by slim tube of 3181 psia. The EOS was checked against current gas-to-oil ratio (GOR) by numerically flashing the oil to a GOR of 40 scf/bbl, representing current conditions, and yielded a MMP of 1180 psia. This MMP was fairly close to the experimentally derived MMP from slim tube of 1400 psia. Since the EOS closely matched both the original oil and depleted oil, it was deemed that this was an acceptable EOS for both matching historic production and for performing predictive simulations.

A simulation model was clipped from the full-field 3-D model and included the Phase 1 and immediately adjacent area. The previously described seven-component EOS was utilized along with the appropriate well completion data for all the wells in the simulation model. This model was then history-matched to the 46 years of production and injection data to validate the model and to get a good estimate of the current saturations and pressures in the model.

Both the Phase 1 area, and wells within it, were matched to oil rate, water cut, and GOR by using individual well liquid rate production and injection rates and bottomhole pressure constraints. Historic pressure was also matched; however, over much of the 46-year history, there were no pressure data to match. At the end of history matching, the Phase 1 area and most wells within it matched the historic data very well, and the model was then used to do predictive simulations.

Six predictive simulation cases were run to evaluate water alternating gas (WAG), continuous CO_2 injection, two injection bottomhole pressure constraints, and varying WAG cycle length. The predictive simulation results indicate that the WAG process yields a faster oil recovery and better sweep efficiency and is more effective than continuous CO_2 injection for recovering hydrocarbon in the Phase 1 area. The earliest CO_2 breakthrough at a production well occurred 3 months after the start of CO_2 injection for continuous CO_2 flooding scenario, while the earliest CO_2 breakthrough with WAG occurred after 2 months. The simulation results also indicated that injected CO_2 is expected to reach 05-06 OW (observation well) 6 months after injection for the continuous CO_2 flooding scenario and 5 months after for the WAG process.

The estimated incidental CO_2 storage potential varied from 3.17 million tons of CO_2, with three hydrocarbon pore volumes (HCPV) of continuous CO_2 injection, to 1.60 million tons of CO_2 with 3 HCPV (1.5 HCPV of CO_2) of 1-to-1 WAG injection.

Future modeling and simulation work on the Bell Creek oil field will include building a Version 3 geocellular model utilizing newly acquired 3-D seismic data, pulsed-neutron logs, and log and core data and include history matching and running predictions on both the Phase 1 and Phase 2 areas.

The information and results presented within this annually updated report represent work performed by the EERC as part of the PCOR Partnership Program. The content represents the authors' views and interpretations at the time the report was written. However, in keeping with the EERC's adaptive management approach, the geologic model and simulations are iteratively updated as new information becomes available. As a result, future versions of Deliverable D66 may contain new data and interpretations that may supersede the information within this report.

BELL CREEK TEST SITE – SIMULATION REPORT

INTRODUCTION

The Plains CO_2 Reduction (PCOR) Partnership, led by the Energy & Environmental Research Center (EERC), is working with Denbury Resources Inc. (Denbury) to determine the effect of large-scale injection of carbon dioxide (CO_2) into a deep clastic reservoir for the purpose of CO_2 enhanced oil recovery (EOR) and to monitor incidental CO_2 storage at the Bell Creek oil field, which is operated by Denbury Onshore LLC (Figure 1). A technical team that includes Denbury, the EERC, and others will conduct a variety of activities to determine the baseline reservoir characteristics, including predictive simulations of the CO_2 injection. This will facilitate assessment of various potential injection schemes, guide monitoring strategies, and determine the ultimate fate of injected CO_2. Denbury will carry out the injection and production operations, while the EERC will provide support for the site characterization, modeling and simulation, and risk assessment and will aid in the development of the monitoring, verification, and accounting (MVA) plan to address key technical subsurface risks.

The Bell Creek CO_2 EOR project provides a unique opportunity to develop a characterization and predictive modeling workflow for a complex, large-scale (>1 million tons a year) CO_2 EOR operation and to monitor and predict incidental CO_2 storage in an active oil field. To facilitate these activities, a detailed static geologic model (Version 1 model) of the Phase 1 (Unit D) area and its surrounding area was built followed by the construction of a Version 2 model representing a 200-square-mile study area centered on Phase 1. During this reporting period, the following was accomplished:

- Updated introductory and geologic history based on continued literature review, core analysis on historic field core located at USGS CRC (U.S. Geological Survey Core Research Center), and examination of outcrops in the Bear Lodge Mountains of Wyoming.

- Completed Version 2 static geocellular model representing a 200-square-mile area centered on Phase 1 and a smaller model of the Phase 1 area clipped from the Version 2 model.

- History matching and predictive simulations were performed to aid in the ongoing planning of various pre- and postinjection monitoring activities in the Phase 1 area.

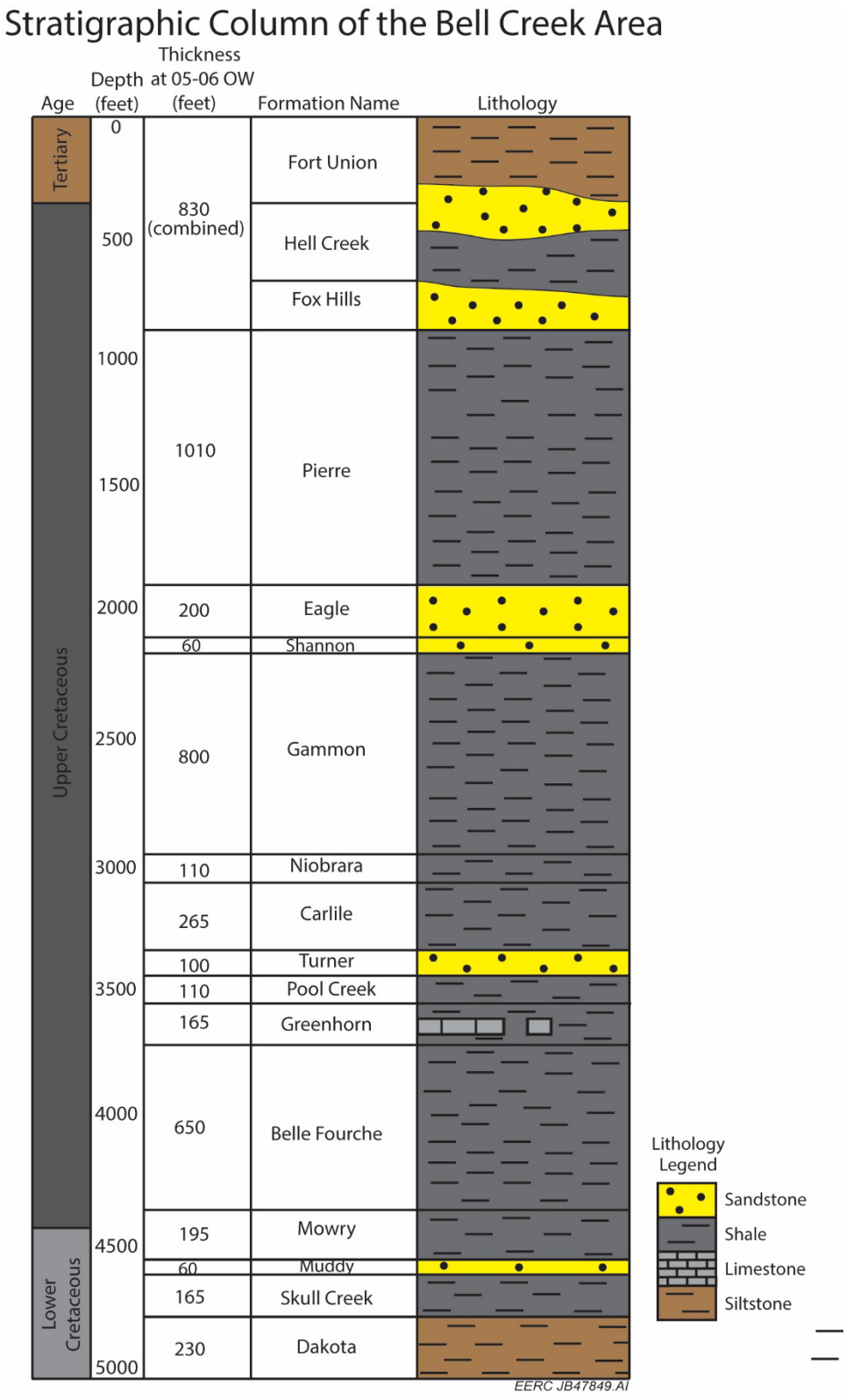

Figure 1. Lower Cretaceous to Quaternary stratigraphic column of the Powder River Basin, as described from the 05-06 OW geologic drilling report.

Future work to be performed is as follows:

- Complete Version 3 static model utilizing newly acquired 3-D seismic data, 35 baseline pulsed-neutron logs, and any additional log and core data derived from newly drilled wells.

- Perform joint simulation of the Phase 1 and 2 areas.

- Model relative permeability hysteresis and CO_2 solubility in the aqueous phase for better estimates of CO_2 breakthrough times and storage capacity.

A new fieldwide static geologic model (Version 2) has been constructed using the fieldwide geologic and reservoir data (Figure 2). The history-matching and predictive simulation results obtained with the Version 1 static geologic model have provided valuable insights about the geologic and reservoir characteristics of the Phase 1 area, which have been incorporated into the Version 2 static model. The baseline geologic characterization and simulation work that will be conducted over the course of this project will also provide valuable data to support the design and implementation of a monitoring program to track the injected CO_2 in the Bell Creek Field.

PURPOSE

The PCOR Partnership is developing a philosophy that integrates site characterization, modeling, simulation, risk identification, and MVA strategies into an iterative process to produce meaningful results for large-scale CO_2 storage projects (Figure 3). Elements of any of these activities play a crucial role in the understanding and development of the others. The modeling and simulation activities described in this report were developed to 1) identify areas where more site characterization data are needed, 2) aid in the identification of potential subsurface risks such as out-of-zone fluid migration, and 3) help in the development of effective monitoring strategies. This integrated process will be refined through each incremental stage of the project, from initial planning, to injection, and through postclosure.

The EERC's geologic modeling of the subsurface assists in understanding and predicting the behavior of the injected CO_2 and reservoir fluids over the injection and postinjection period. To aid in the validation of the reservoir model, history matching is performed on a numerically tuned dynamic reservoir model that is constructed using a completed 3-D static geologic model. This is followed by simulation work, which is a valuable tool for assessing scenarios of fluid migration within the reservoir and the potential for out-of-zone fluid migration. Additionally, simulation activities provide a means to evaluate the sweep and storage efficiency and the applicability of various monitoring activities related to both incidental CO_2 storage and CO_2 EOR.

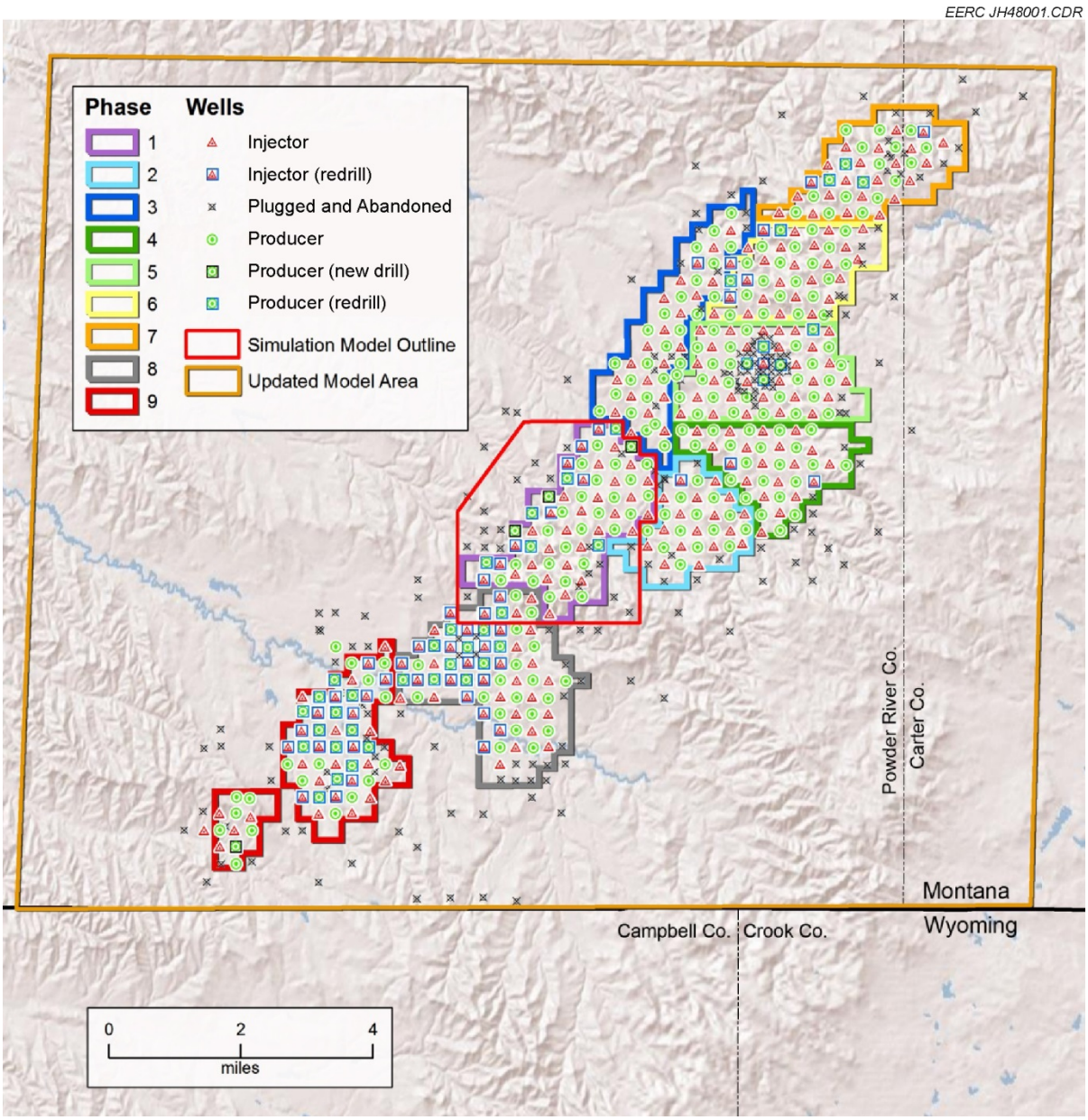

Figure 2. Study area for the fieldwide 3-D geologic model (orange), showing the simulation model outline (red).

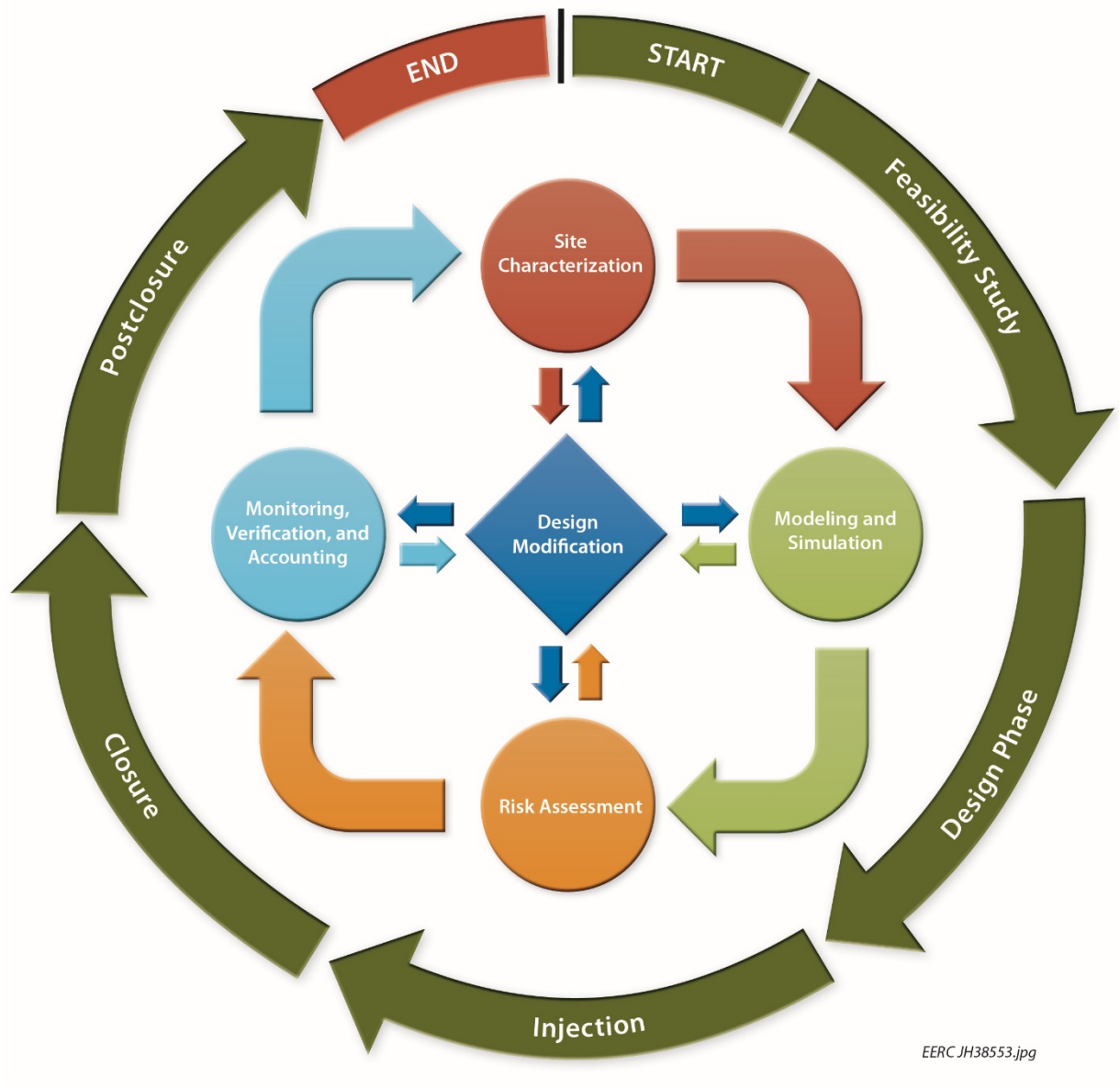

Figure 3. Project elements of the Bell Creek CO_2 capture and sequestration project. Each of these elements feeds into another, iteratively improving results and efficiency of evaluation.

Performing geologic characterization, geocellular modeling, and numerical simulation is essential input for risk identification and to guide MVA. This approach lays the foundation for a project-specific, risk-based, goal-oriented MVA plan. The goal of the MVA plan is to effectively monitor the behavior of the injected CO_2 and reservoir fluids in the subsurface throughout the project life. Predictive simulations allow for targeted deployment of MVA data acquisitions at optimal geographic locations and time intervals to maximize the knowledge gained and minimize expenditures. The results and experience gained at the Bell Creek oil field will provide insight and knowledge that can be directly and readily applied to similar projects within the PCOR Partnership region and throughout the world.

SCOPE OF WORK

In order to evaluate the efficiency of large-scale CO_2 injection for CO_2 EOR and to monitor incidental CO_2 storage in the Muddy Formation of the Bell Creek oil field, several iterations of a 3-D geologic model coupled with dynamic simulation work were completed. The first static geologic model of the Phase 1 area (the Version 1 model) has been completed along with subsequent history matching and a few predictive simulation scenarios. Further predictive fluid flow simulations are being conducted to more accurately model CO_2 propagation in the subsurface. This allows for targeted monitoring activities and a means of theoretically evaluating various injection scenarios for oil recovery and incidental CO_2 storage. Based on the insights gained from the Version 1 model, a second iteration representing the entire field (Version 2 model) was created using updated characterization data performed on the reservoir and outcrop.

Extensive data reconnaissance was performed to fully evaluate both current and anticipated reservoir behavior, original oil in place (OOIP), incremental production assessments, and the ultimate fate of injected CO_2 through geologic modeling and dynamic simulations. Available data were analyzed, interpreted, and incorporated into the 3-D static geologic and dynamic reservoir models to represent geologic and reservoir properties in order to provide a solid groundwork for simulation activities. Furthermore, what was learned from construction and simulation of the Phase 1 geologic model was carried over into the fieldwide geologic model, which is more robust and less uncertain in several areas because of the incorporation of new and refined knowledge.

BACKGROUND

The Bell Creek oil field in southeastern Montana is a subnormally pressured reservoir with significant hydrocarbon charge that lies near the northeastern boundary of the Powder River Basin (Figure 4). Exploration and production activities for mineral and energy resources in the area over the last 55 years have yielded a significant amount of information about the geology of southeastern Montana and the northern Powder River Basin which has been cataloged in a literature review. Decades of oil and gas production through primary and secondary recovery (waterflood and polymer flood pilot tests) have resulted in reservoir decline and have now led to the planned implementation of a CO_2 injection-based tertiary oil recovery project. CO_2 will be delivered to the site via a 232-mile pipeline from the ConocoPhilips Lost Cabin natural gas-processing plant, where it is separated from the process stream during refinement of natural gas (Figure 4). The Lost Cabin plant currently generates around 50 million cubic feet of CO_2 a day.

CO_2 will be injected into the oil-bearing sandstone reservoir in the Lower Cretaceous Muddy (Newcastle) Formation at a depth of approximately 4500 feet (1372 meters). Nine stages of injection are scheduled to occur across the field. It is expected that the reservoir will be suitable for miscible flooding conditions with an incremental oil production target of approximately 30 million barrels. The activities at the Bell Creek oil field will inject an estimated 1 million tons of CO_2 annually, much of which will be permanently stored at the end of the EOR project.

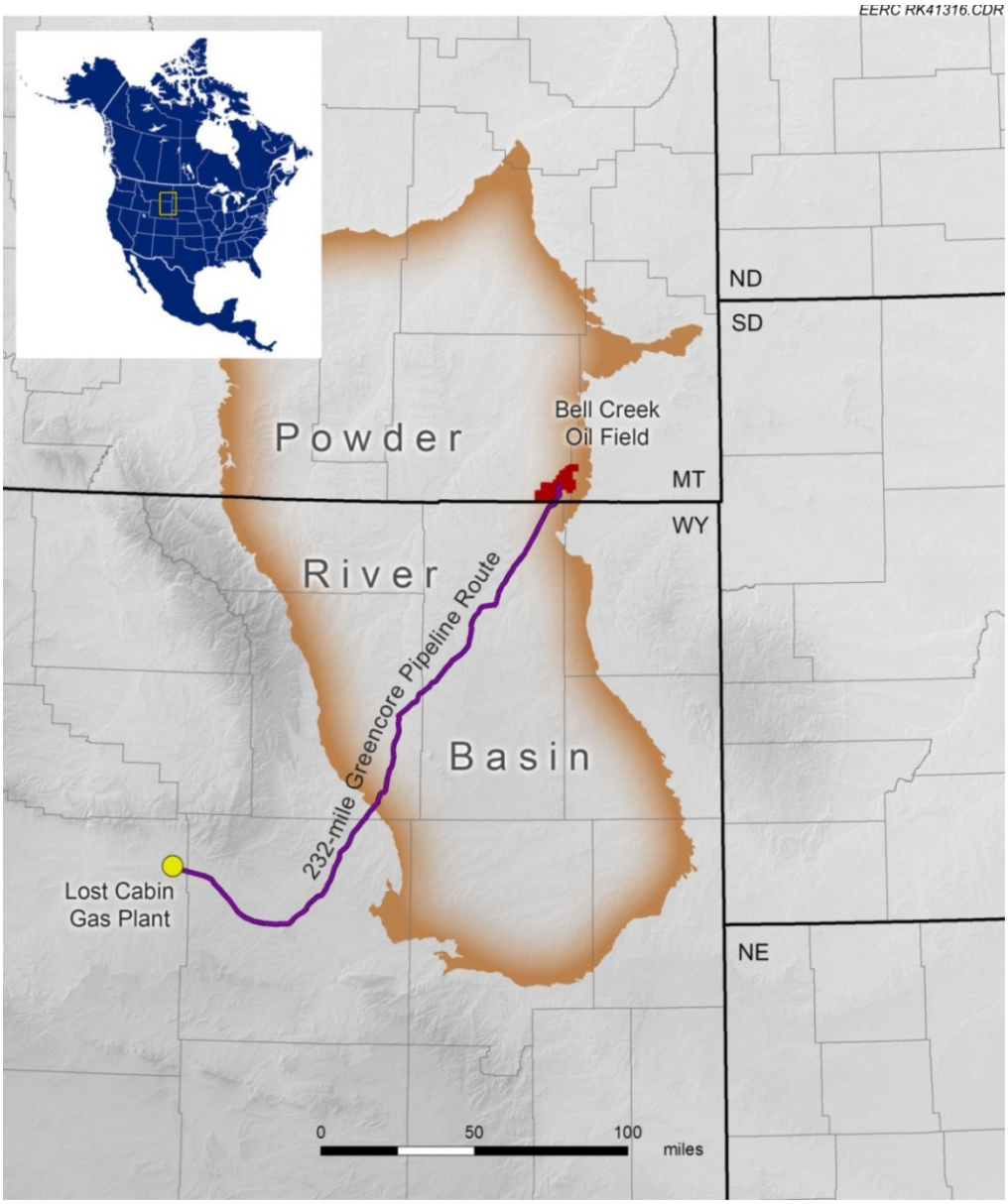

Figure 4. Map depicting the location of the Bell Creek oil field in relation to the Powder River Basin and the completed pipeline route to the site from the Lost Cabin gas plant.

Within the Bell Creek oil field, the Muddy Formation is dominated by high-porosity (25%–35%), high-permeability (150–1175 mD) sandstones deposited in a near-shore marine environment (Saini and others, 2012). The initial reservoir pressure was approximately 1200 psi, which is significantly lower than the regional hydrostatic pressure regime (2100 psi at 4500 ft). The oil field is located structurally on a shallow monocline with a 1°–2° dip to the northwest and with an axis trending southwest to northeast for a distance of approximately 20 miles. Stratigraphically, the Muddy Formation in the Bell Creek oil field features an updip sand facies pinchout into shale facies serving as a trap. The barrier-bar sand bodies of the Muddy Formation strike southwest to northeast and lie on a regional structural high, which represents a local paleo-

drainage deposition. A deltaic siltstone overlaps the sandstone on an erosional barrier-bar surface and finally is partially dissected and somewhat compartmentalized by intersecting shale-filled incisive erosional channels.

The overlying Lower Cretaceous Mowry Shale provides the primary seal, preventing fluid migration to overlying aquifers and to the surface. On top of the Mowry Shale are several thousand feet of low-permeability formations, including the Belle Fourche, Greenhorn, Niobrara, and Pierre Shales, which will provide redundant layers of protection in the unlikely event that the primary seal fails to prevent upward fluid migration fieldwide (Figure 2).

GEOLOGIC HISTORY

The Muddy Formation within the boundaries of the Bell Creek oil field comprises a near-shore marine barrier-bar sequence that was deposited in the Albian Age of the Cretaceous Period (Figure 5), approximately 99 million years ago. Several transgressive and regressive sequences occurred during the Lower Cretaceous, depositing the entire system seen within the Muddy Formation. At the base of the Muddy Formation lies the Skull Creek Shale which was deposited in an offshore marine environment where copious amounts of clay material could accumulate over an extensive time period. The Skull Creek was the direct result of sea rise southward across the Western Interior during the early Albian Age (Figure 6). This southward transgression continued and eventually joined the northward-transgressing Gulf Sea. At its maximum transgression, the Early Cretaceous seaway covered most of Montana, North Dakota, South Dakota, Wyoming, Colorado, Kansas, and much of western Nebraska (Figure 6) (Vuke, 1984; Young, 1970).

The sea began a major regression northward during the middle Albian (Figure 7). This regression exposed the Skull Creek to subaerial erosion and caused the formation of large deltas and major drainage systems that cut deep channels into the Skull Creek Shale. These regressive deltaic and fluvial deposits make up much of the lower part of the Muddy Sandstone (Wulf, 1962). The Muddy Sandstone are Lower Cretaceous Albian-age rocks deposited in western North Dakota and southwestern Montana, respectively (Figure 5). Weimer and others (1982) interpret variations in thickness and lithology within the Muddy Formation as being caused by recurrent movement on basement fault blocks, influencing the location and pattern of the incised valleys. Evidence of the regressing shoreline can be found as far north as southern Montana (Vuke, 1984). This major regression and maximum lowstand of the sea combined with the subsequent and future transgression allowed deltaic sediments to be reworked into beaches, offshore bars, and barrier bars.

The sea began to transgress south again during the late Albian (Figure 8). This transgression eroded and reworked the previous deltaic sands, forming a major unconformity, and subsequently deposited Coastal Plain sequence overlying the Muddy Sandstone. Valleys incised into the Coastal Plain were also filled with marine sands and muds. As the sea deepened during another dominant transgressive stage, it began to deposit the thick marine shales of the Mowry Formation on top of the Muddy Formation.

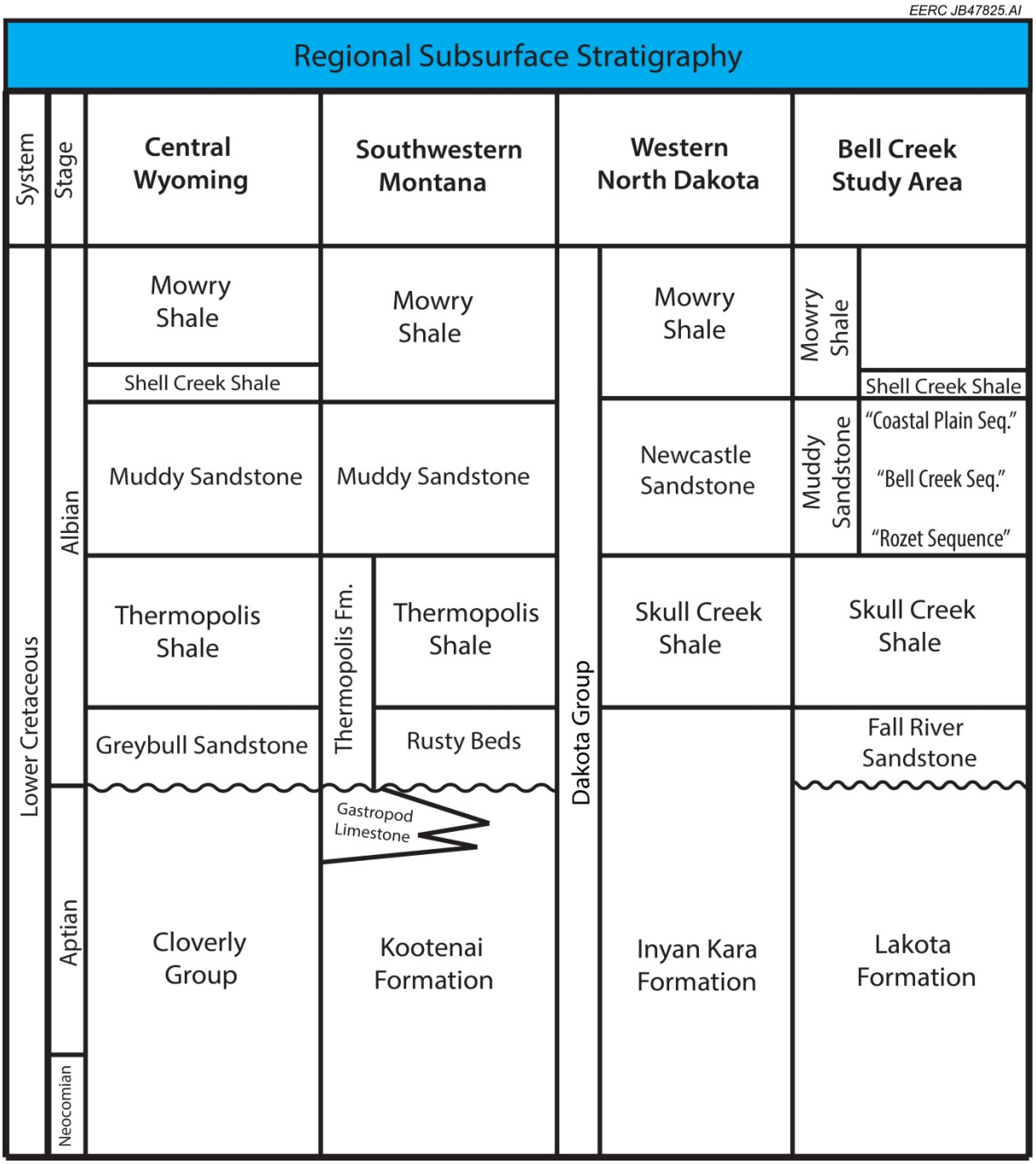

Figure 5. Stratigraphic column of the Lower Cretaceous series. The Bell Creek study area column contains the nomenclature used in this report (modified from Vuke, 1984).

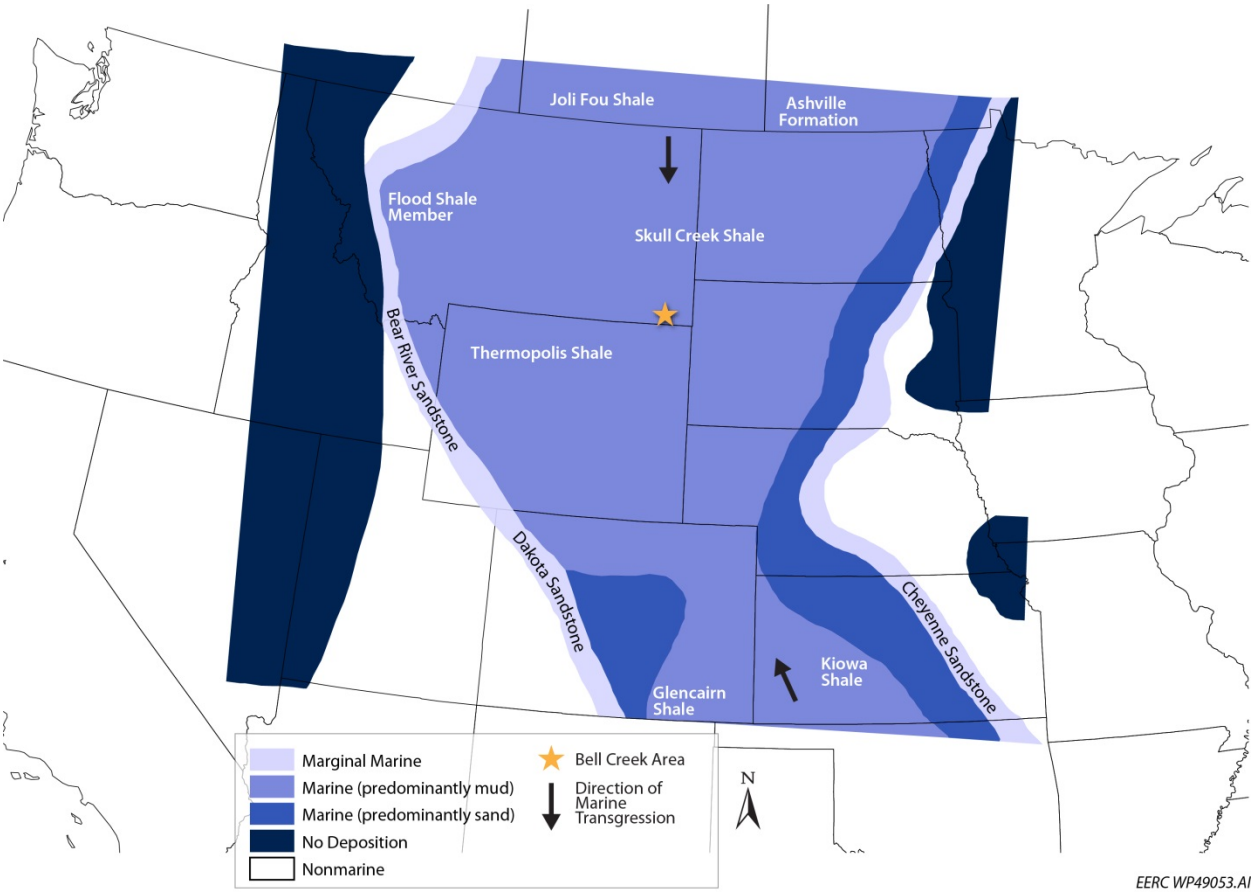

Figure 6. Maximum transgression of the Early Cretaceous seaway, showing deposition of the Skull Creek Shale (modified from Vuke, 1984).

Local Depositional Environments

The Muddy Formation comprises, in descending order, the Coastal Plain sequence, the Bell Creek Sandstone sequence, and the Rozet sequence (Figure 5). The Muddy Formation is stratigraphically positioned between the thick marine shale sequences of the Skull Creek and Mowry Formations. Within the field, the Muddy Formation has an average depth of 4500 ft and dips to the northwest at about 1°–2°. The nomenclature for the sequences within the Muddy Formation has changed over time and is regionally variable.

The Rozet sequence directly overlies the Skull Creek Shale and is marked by a thin (0.5–3-ft) hummocky cross-stratified sandstone bed, which is conformably overlain by a dark gray mudstone. This sequence was deposited in an offshore marine environment and marks a basinward shift in facies, correlating to the first major regression of the Western Interior Seaway that deposited the Skull Creek Shale, as described above. After a minor rise in sea level, corresponding to the dark gray mudstone at the top of the Rozet Sequence, sea level began to fall again (regression).

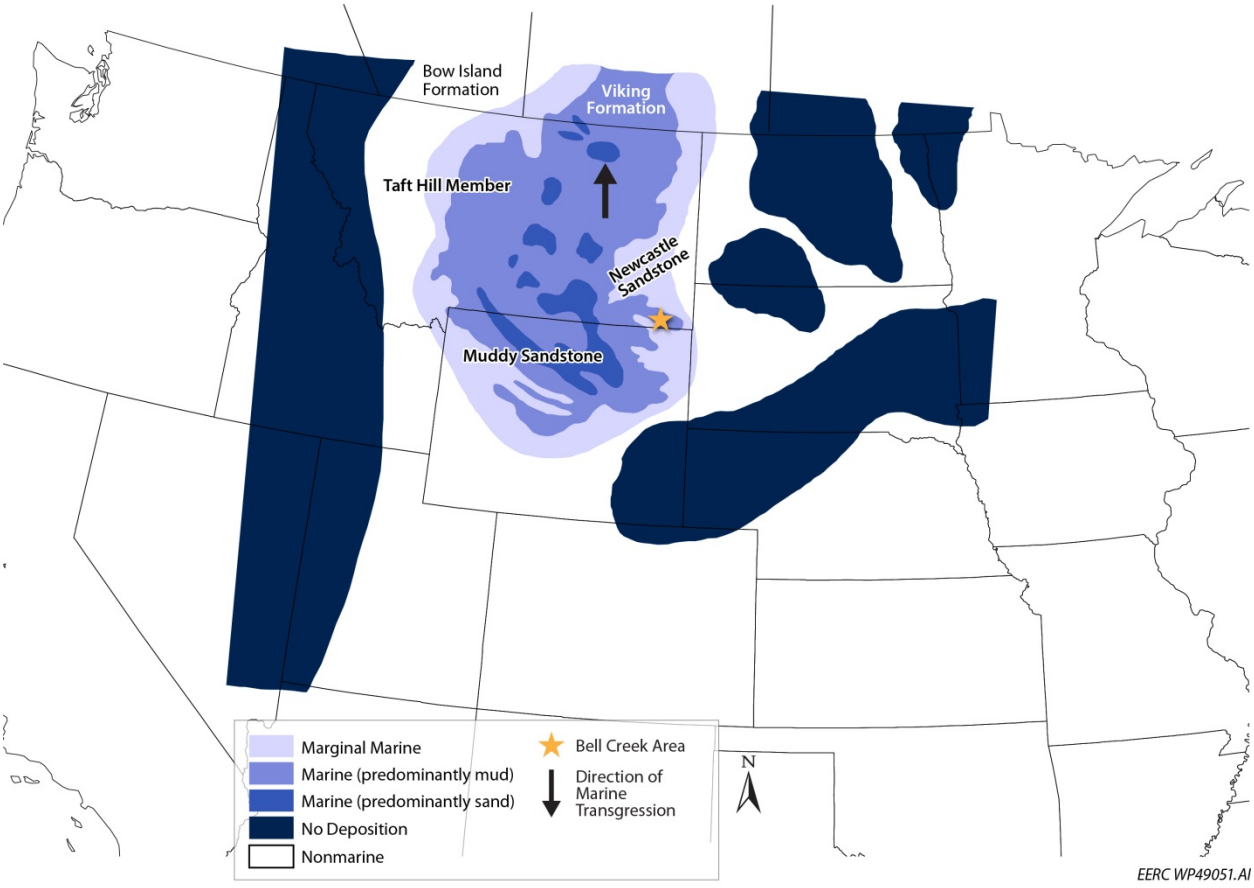

Figure 7. Regression of the Early Cretaceous seaway deposited the Muddy Sandstone (modified from Vuke, 1984).

As sea level continued to fall, large deltas and drainage systems began to form and cut channels into the Skull Creek Shale. The Bell Creek sequence is made up of stacked barrier-bar sediments that were reworked and transported by longshore drift from these drainage systems. The barrier-bar sands of the Bell Creek sequence make up the best reservoir rock within the field. These sediments intertongue with marine shales to the west-northwest and lagoonal sediments to the east-southeast, representing minor changes in sea level during deposition. This facies change updip to the east and southeast provides the trapping mechanism to allow pooling of hydrocarbons in the barrier-bar sandstones.

The Coastal Plain sequence lies unconformably on the Bell Creek sequence. It was deposited when another drop in sea level caused the incision of fluvial channels into the Bell Creek sequence, some of which cut down to the Skull Creek Shale. These channels, oriented mainly east–west, were filled with fluvial sandstone, floodplain shale, coal, and marginal marine deposits during the subsequent rise in sea level. This sea-level rise corresponds to the early stages of the major transgression that led to the deposition of the Mowry Shale.

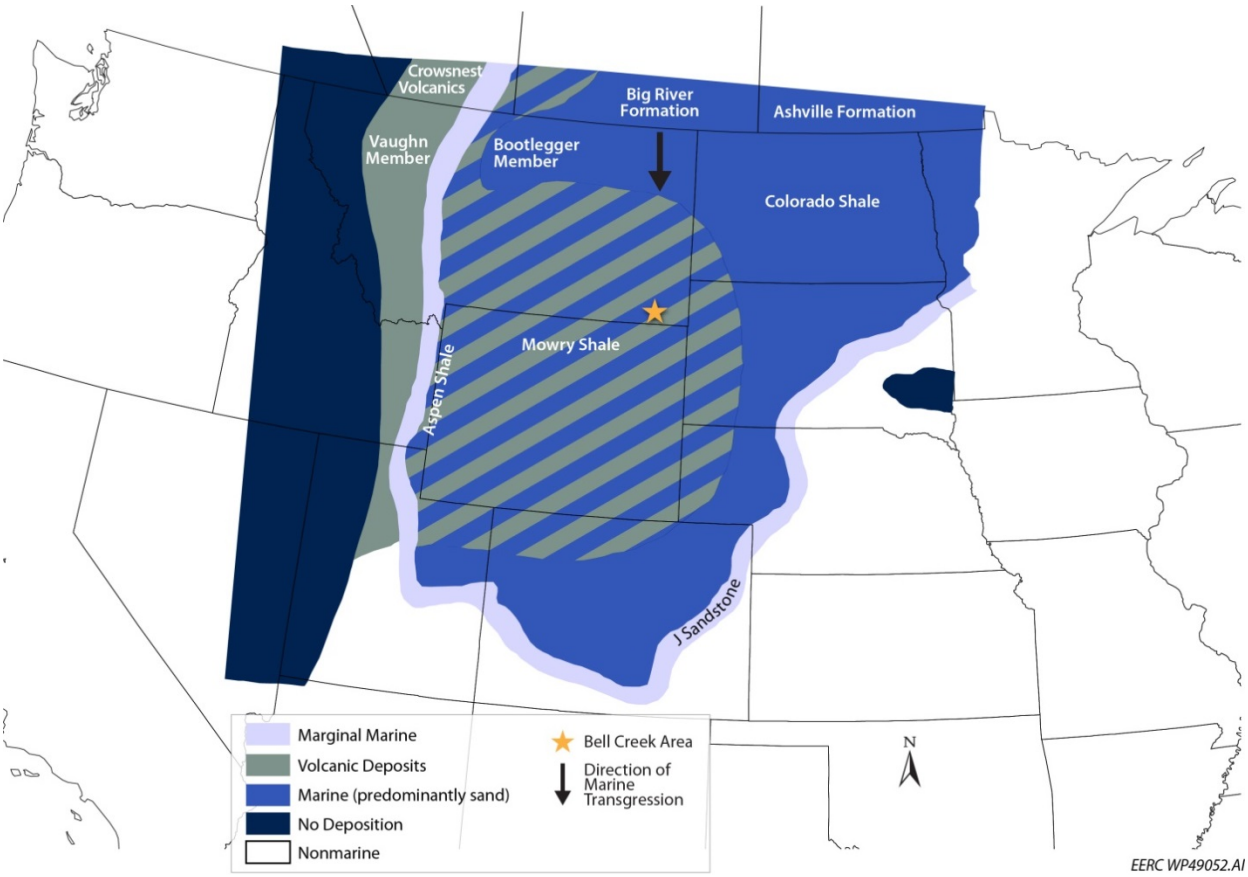

Figure 8. Transgression of the Early Cretaceous seaway, which deposited the Mowry Shale (modified from Vuke, 1984).

3-D GEOLOGIC MODELING

Advanced 3-D geologic modeling utilizing Schlumberger's Petrel® software has been conducted in order to characterize the geologic framework of the Muddy Formation within the geologic model boundary that is underlain by Skull Creek Shale and overlain by Mowry Shale. Three versions of the geologic modeling have been constructed or are under construction. Version 1 was completed in 2012 and had a study area focused around Phase 1 of the Bell Creek Field. Version 2 was completed in 2013 with a much larger fieldwide study area and is presented herein. Version 3 is currently ongoing and will be reported in the future work section.

To construct a detailed fieldwide 3-D static geologic model (Version 2), fieldwide data reconnaissance activities were performed to acquire pertinent reservoir characterization data for the entire Bell Creek oil field, while still focusing more on the Phase 1 area as injection activities will begin there. Since oil activity has been prolific in the past, an abundance of vintage geologic data exists in the form of geophysical well logs, lithology descriptions from well files, geologic maps, core data analysis, and cross sections. These data combined with detailed geologic interpretation of petrophysical and lithological facies aided in the creation of a detailed structural framework across the 200-sq-mile study area.

Inside this study area are 748 wells with geophysical logs and 94 wells with preserved 2.5- to 4-in. cores. In addition, a wealth of geologic, geomechanical, and reservoir properties has been acquired from the 05-06 OW monitoring well (Figure 9). A suite of 11 geophysical logs have been used to correlate with the historical log suite for use in normalization, stratigraphic, facies, and petrophysical workflows.

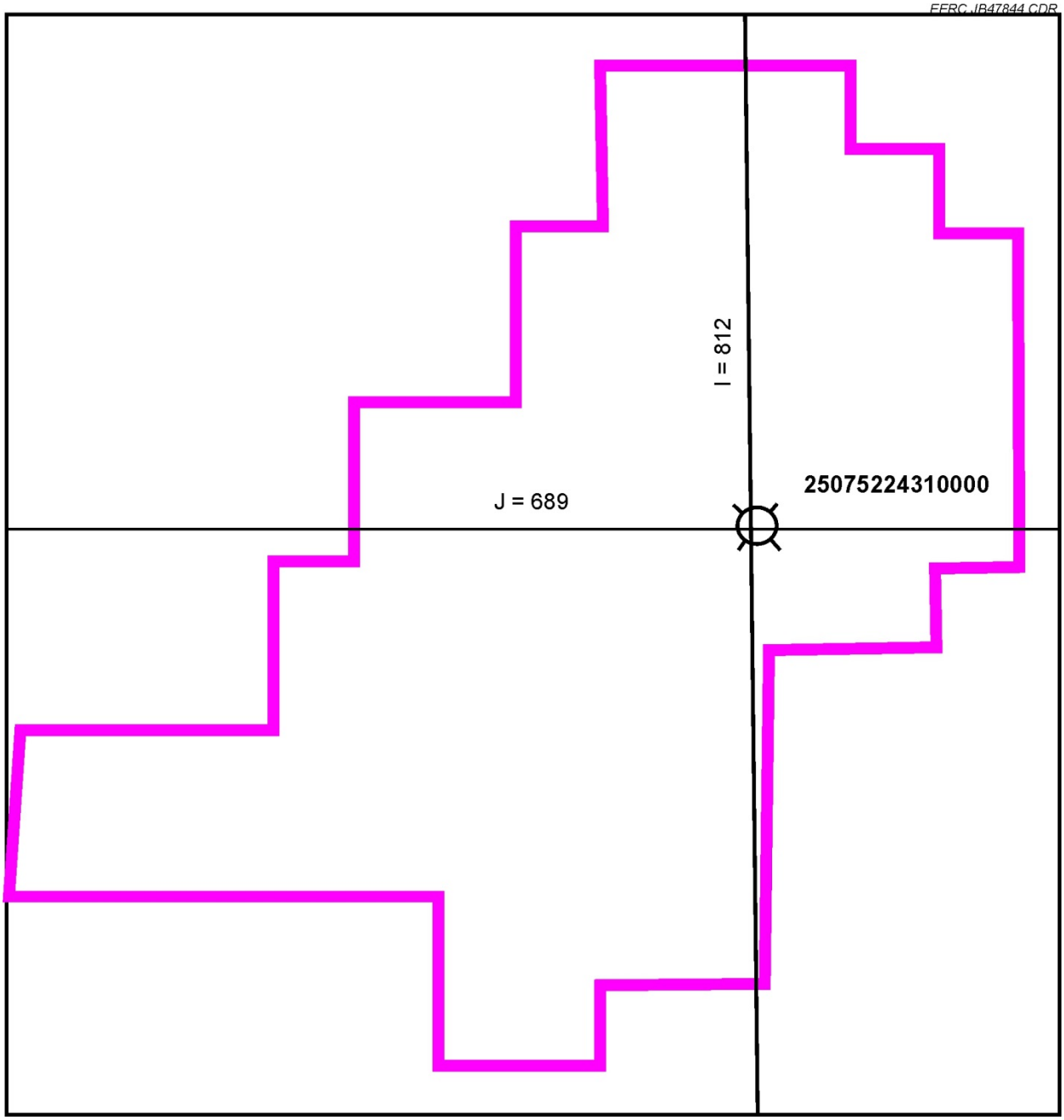

Figure 9. Phase 1 boundary showing the location of the 05-06 OW (25075224310000) and two cross-section lines (J = 689 and I = 812) that will be referred to for visual analysis of the 3-D geologic model.

The 3-D geologic model was constructed to incorporate a distribution of facies followed by petrophysical properties conditioned to the facies. The following facies were first assigned to six type well logs with subsurface core available for calibration purposes and then distributed to the remaining wells in the study area using a batch processing workflow in Schlumberger's Techlog:

- Mudstone/siltstone
- Shale
- Poor reservoir sand
- Good reservoir sand
- Silty sandstone

Upon distribution of facies to the well logs, a geostatistical workflow populated the 3-D model's structural framework with a facies property. The following petrophysical properties were then assigned geostatistically throughout the model according to facies type:

- Shale volume
- Total porosity
- Effective porosity
- Permeability
- Net-to-gross
- Water saturation

The geologic framework and assigned properties conditioned to facies, along with temperature and pressure properties, are necessary components for performing dynamic flow simulations that aid in estimating incidental CO_2 storage and EOR efficiencies, estimating CO_2 breakthrough time at various production wells, studying the long-term CO_2 plume and pressure behaviors and ultimate fate of injected CO_2. Various predictive simulation scenarios also provide necessary inputs for preparing and enhancing a monitoring program to track CO_2 movement in the reservoir through targeted monitoring activities.

Stratigraphic Framework

Six zones make up the Version 2 model stratigraphy and were picked across all 748 wells culminating in over 4400 individual tops (Figure 10). Structural surfaces were interpolated using top depths in a detrending and geostatistical workflow. P10, P50, and P90 realizations were created for the Bell Creek sandstone structural top, and the P10 was then subtracted from the P90 to show uncertainty ranges (Figure 11). Since the uncertainty range was minimal within the field, the P50 surface was used going forward. All other remaining structural surfaces were interpolated using the P50 Bell Creek sandstone as a trend surface. A generic surface 30 feet below the top of the Skull Creek Formation was created to represent the basal zone and cap rock below the reservoir. This was done to limit unnecessary cap rock layers and reduce overall cell count in the reservoir model. Isopachs were generated between the surfaces and examined for inconsistencies and surface crossover.

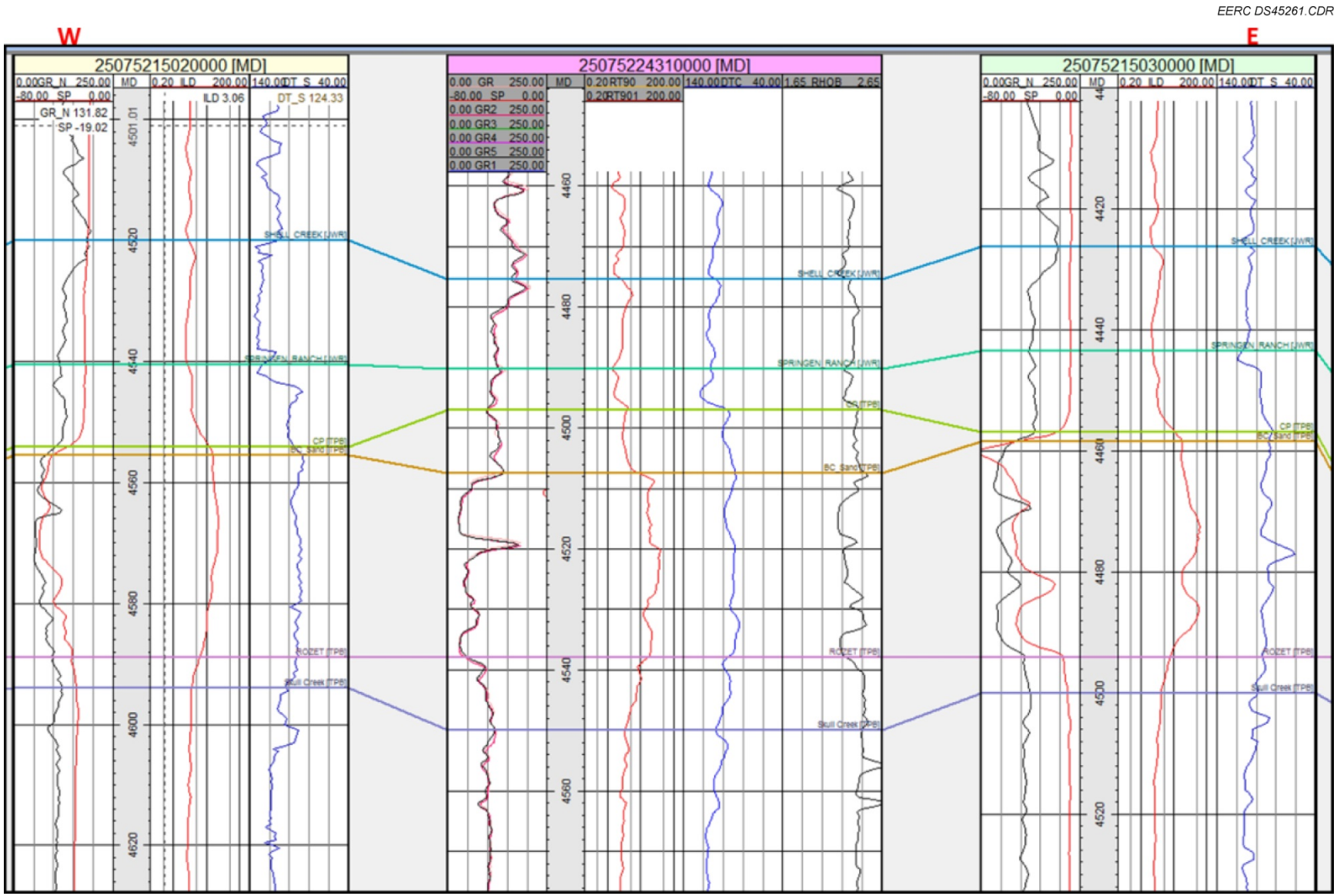

Figure 10. West-to-east cross section through wells nearest to and including the 05-06 OW (25075224310000). Six structural tops are shown in descending order: Shell Creek, Springen Ranch, Coastal Plain, Bell Creek, Rozet, and Skull Creek.

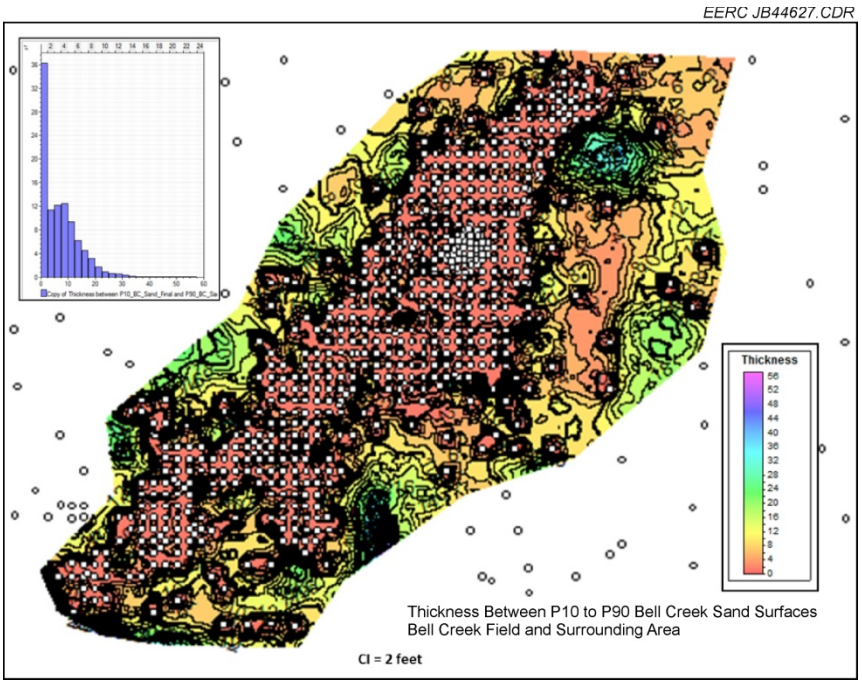

Figure 11. Uncertainty range of probabilistic structural surfaces of the Bell Creek oil field.

Structural Model

The 3-D structural model was created using the six interpolated structural top surfaces, the extent of the study area, and a cell size of 50 ft × 50 ft. These six correlated surfaces plus an additional basal surface placed at 30 feet below the Skull Creek top represent the six zones within the model (Figure 12): Shell Creek, Springen Ranch, Coastal Plain, Bell Creek Sandstone, Rozet, and Skull Creek. These six zones have been further subdivided into finer layers to help capture the heterogeneity within the facies and associated reservoir properties (Table 1). Thus 39 vertical layers exist in the model, resulting in just over 100 million cells represented in the Version 2 static geocellular model.

Facies Model

To better assign petrophysical properties inside the structural model, a facies workflow was followed to condition facies to logs, followed by population into the model geostatistically. Six type wells were chosen across the study area for training wells in facies analysis using Techlog's Ipsom module. Using the six wells, five facies classes were defined: mudstone/ siltstone, shale, poor reservoir sand, good reservoir sand, and silty sandstone. The wells were populated with the five facies based on a specific range of the following logs: resistivity, gamma ray, and bulk density. These numerically derived facies were then checked against macro lithofacies descriptions from subsurface core for uncertainty analysis (Figure 13). After core-to-log calibration of the type logs, a batch process was used to calculate facies logs in the remaining wells in the study area that had, at minimum, resistivity, gamma ray, and bulk density logs. This was followed by geostatistically populating the facies into the 3-D structural model (Figure 14).

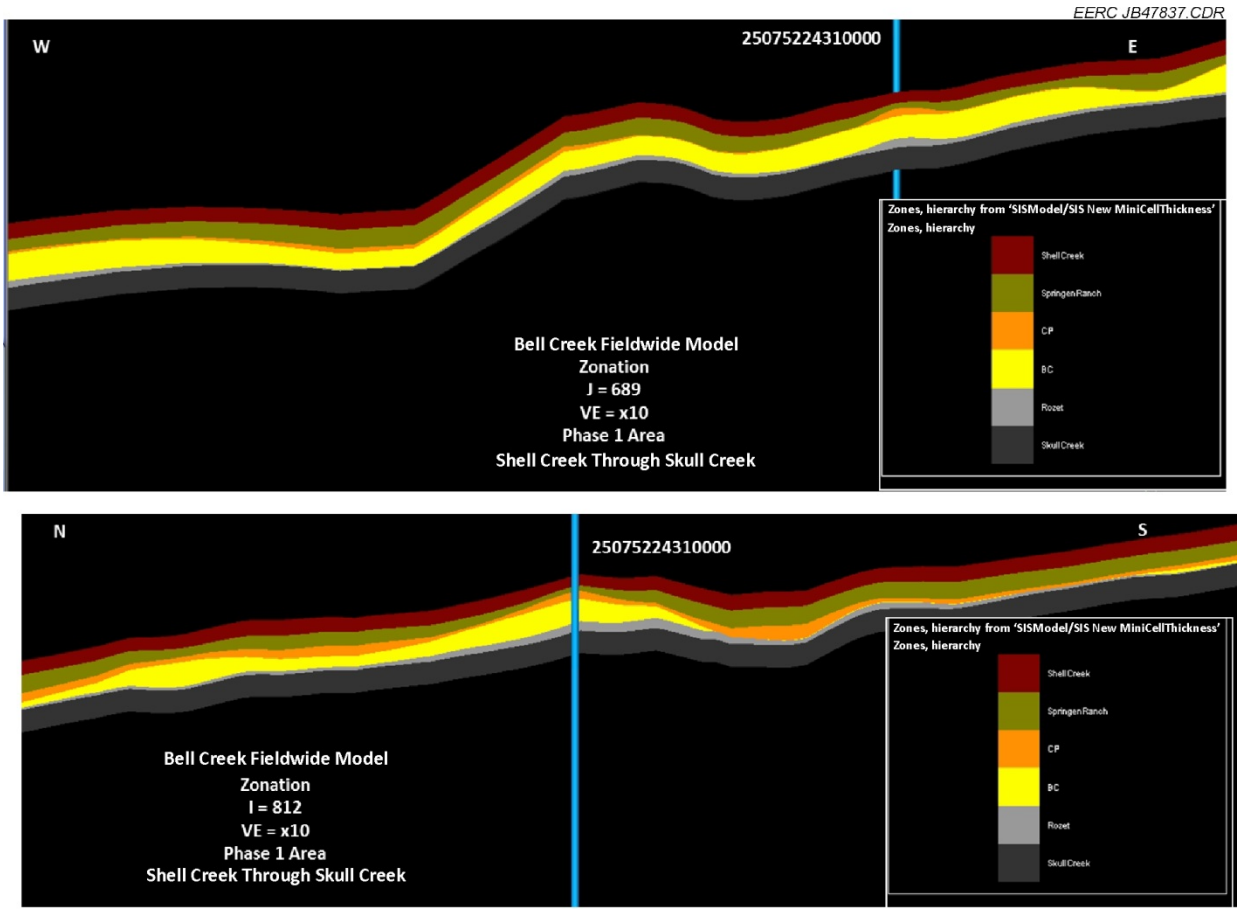

Figure 12. Version 2 geologic model zonation cross sections through the Phase 1 area. Refer to Figure 9 for a map view of the sections; the 05-06 OW is shown.

Table 1. Layers and Associated Thicknesses of Stratigraphy in the Fieldwide Geologic Model

Bell Creek 2012 Fieldwide Model Gridding, 50-ft × 50-ft Grid Dimension				
Zone	Number of Layers	Layer Numbers	Thickness Range, ft	Average Thickness, ft
Shell Creek	3	1–3	2.2–8.3	6.0
Springen Ranch	4	4–7	1.1–11.8	5.0
Coastal Plain	6	8–13	0.2–5.5	1.0
Bell Creek Sand	20	14–33	0–3.3	1.0
Rozet	3	34–36	0.3–5.3	2.0
Skull Creek	3	37–39	10.0	10.0

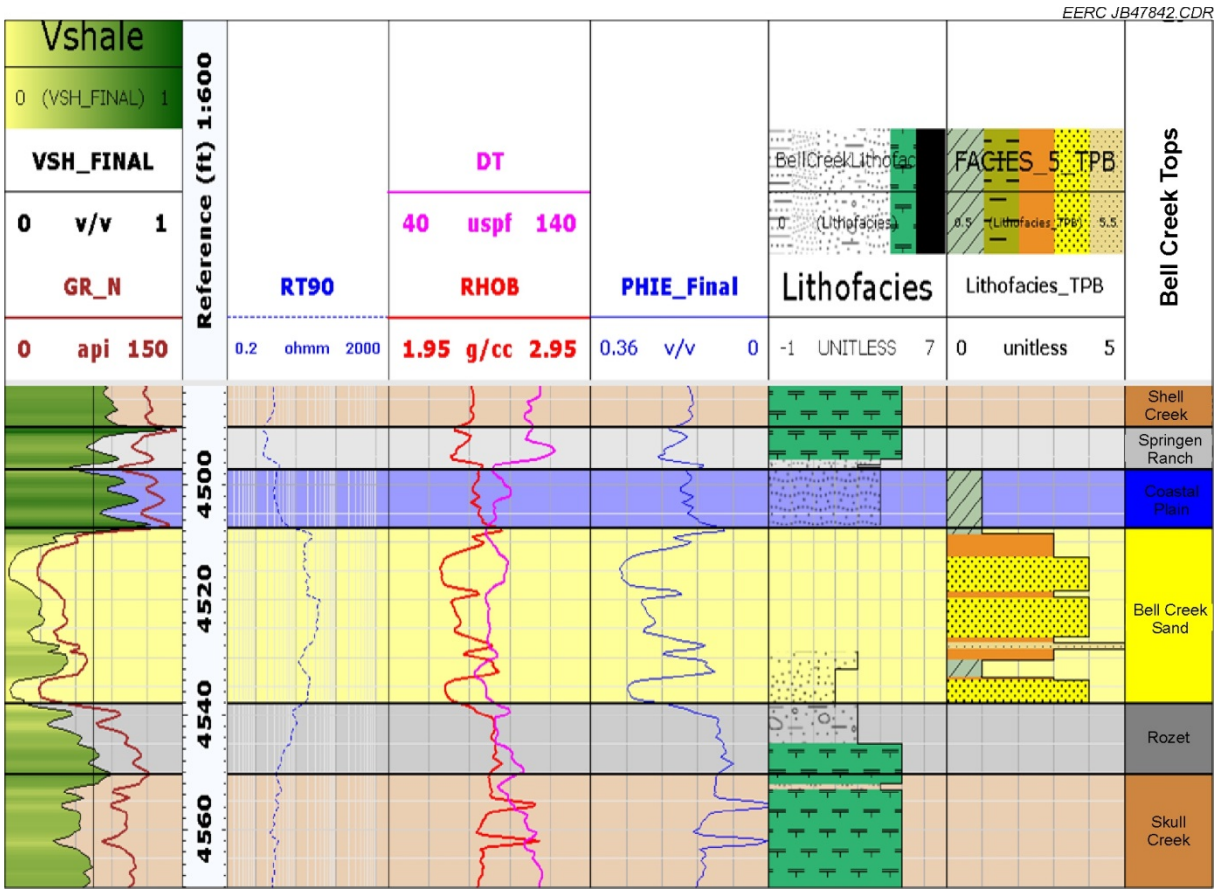

Figure 13. Techlog output showing a type well (05-06 OW) with several logs from left to right: shale volume and normalized gamma ray, depth track, deep resistivity, delta transit time and bulk density, effective porosity, macro core facies, petrophysical facies, and stratigraphic zone.

Petrophysical Model

The following properties were calculated based on geophysical log response and then conditioned to facies before population into the 3-D structural model:

- Shale volume
- Total porosity
- Effective porosity
- Permeability
- Net-to-gross
- Water saturation

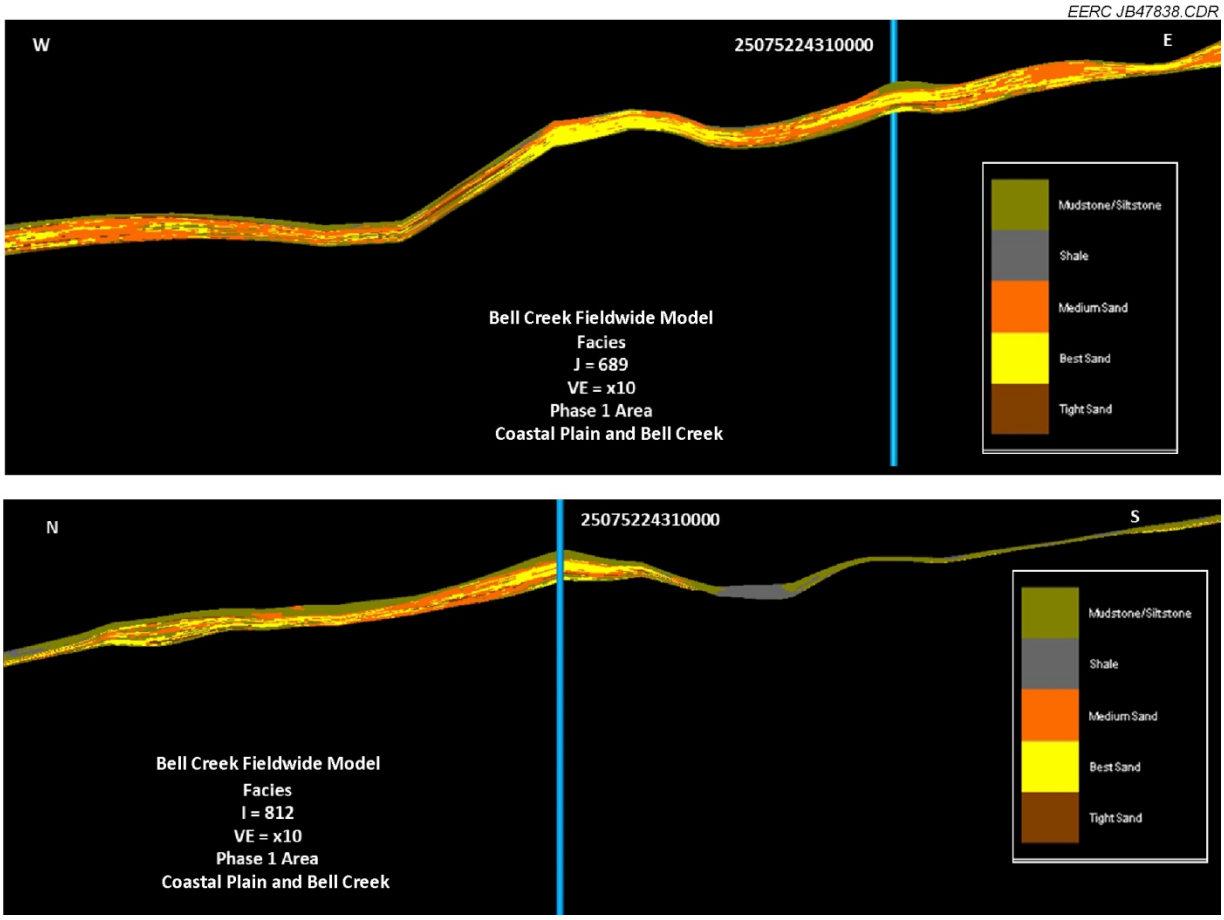

Figure 14. Phase 1 cross sections showing geostatistically populated facies within the 3-D structural model. See Figure 9 for a map view of the sections; the 05-06 OW is shown.

Shale Volume

The shale volume property was created in Techlog first by developing a core shale volume log by taking (1 − % quartz). This curve was then plotted against three different shale volume analysis methods from Techlog. The linear method showed the best results when correlated to the core XRD (x-ray diffraction) results and was used to compute shale volume for all wells within the study area that had a gamma ray log.

Total Porosity

The total porosity log was derived from a combination of core porosity and bulk density porosity. It was noted from *Crain's Petrophysical Handbook* (Crain, 2000) that core-derived porosity is most likely equal to total porosity derived from logs. A crossplot of 100 wells was made to compare core porosity to bulk density-derived porosity. The following formula was derived in order to apply this total porosity designation to all other wells with bulk density logs:

$$PHIT\_Final = 1.033*PHIT\_D + 0.013832$$

Where PHIT_Final is the total porosity log and PHIT_D is the total porosity as derived from the bulk density log.

Since only 381 wells had bulk density logs (Table 2), synthetic logs were computed for the remaining wells using Techlog's neural network module. These synthetic logs were computed using a combination of compressional slowness (DT), deep resistivity (ILD), gamma ray (GR), and shale volume (VSH) logs to create a synthetic bulk density (RHOB-Syn) log for each well (Figure 15). To ensure that the algorithm produces the most realistic synthetic logs, 18 wells that had bulk density (RHOB_S) logs were run through the workflow in order to compare the synthetically derived log to the original log response (Figure 15). In the event the results did not match, the workflow was adjusted and rerun until all 18 wells had good matches. Then the workflow was run on all wells that had bulk density logs to produce synthetic bulk density curves (RHOB-Syn).

Table 2. Number of Wells with DT and RHOB Logs

	DT and RHOB	DT only	RHOB only	No DT or RHOB
No. Wells	130	332	251	35

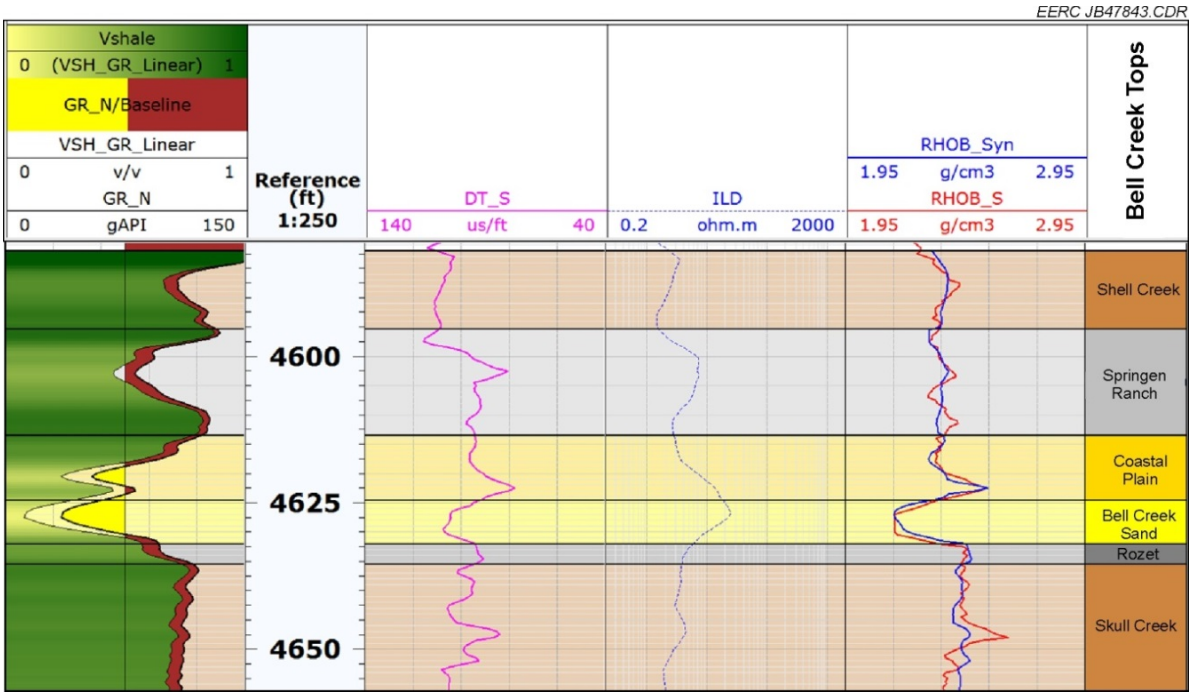

Figure 15. Result and comparison of actual bulk density log vs. the synthetically produced log in Well 25075215140000.

Effective Porosity

Effective porosity was computed by using a combination of the total porosity log, density log, and shale volume log. Two effective porosity properties were created based on different values for shale density. Core shale density was reported to be 2.65 g/cm^3, while log-derived shale density was calculated at 2.4 g/cm^3 and thus reported as $PHIE_{2.6}$ and $PHIE_{2.4}$, respectively. The equation to compute effective porosity is the rock matrix total porosity minus the total porosity of shale multiplied by the volume of shale: PHIE = total porosity rock matrix – (total porosity of shale × volume of shale). Thus an overestimation of the shale density will reduce the overall effective porosity, and an underestimation of the shale density will increase the overall effective porosity. Sample equations are as follows:

$$PHIE_{2.4} = PHIT - (0.04 \times \text{volume of shale}) \quad \text{[Eq. 1]}$$

$$PHIE_{2.6} = PHIT - (0.27 \times \text{volume of shale}) \quad \text{[Eq. 2]}$$

Both equations were utilized and yielded two effective porosity properties that were populated into the 3-D structural model using sequential Gaussian Simulation (SGS) and cokriged with the total porosity property (Figure 16).

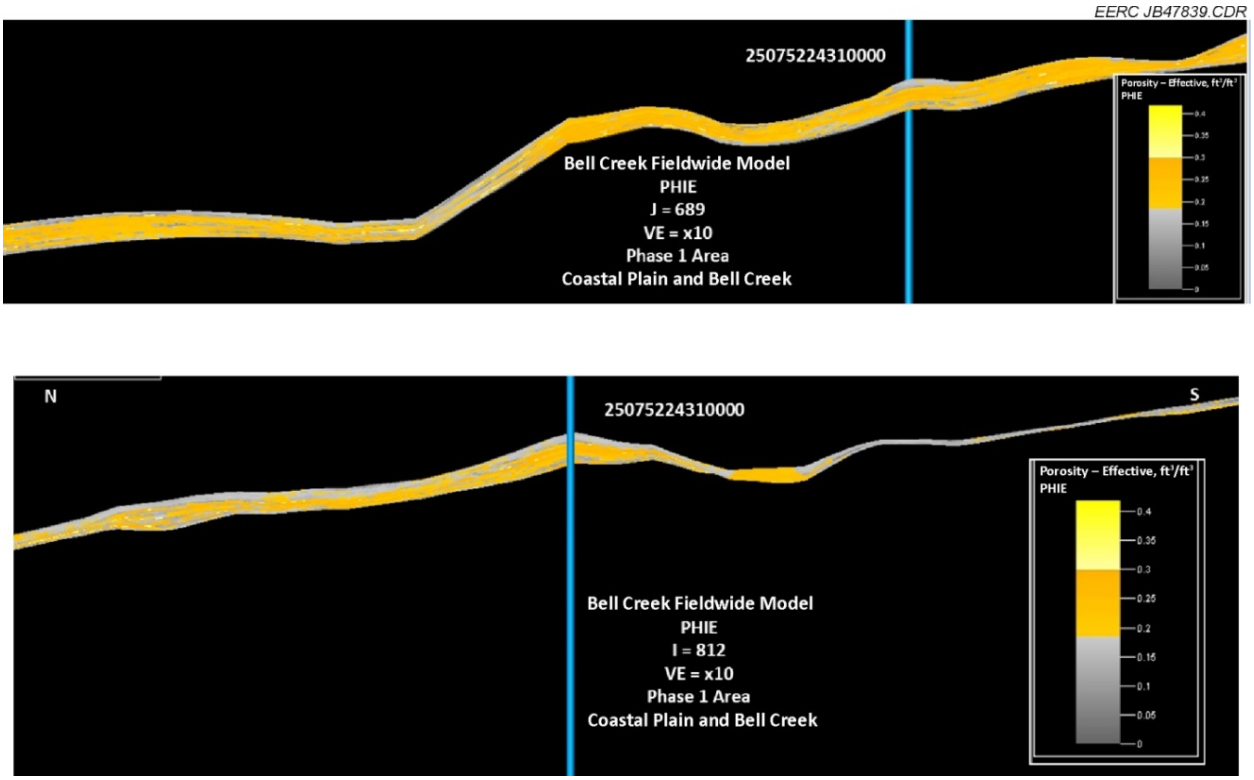

Figure 16. Phase 1 cross sections showing geostatistically populated effective porosity within the 3-D structural model. See Figure 9 for a map view of the sections; the 05-06 OW is shown.

Permeability

One hundred seventy-six wells with data points for core porosity and permeability were loaded into Techlog. Crossplots were built for the Bell Creek sequence, Coastal Plain sequence, and the entire Muddy Formation interval to ensure a valid relationship between the two reservoir properties. Then permeability logs were computed using a neural network workflow in Techlog. Most wells have a strong correlation with bulk density response and neural network-derived permeability and were used to train the module. Wells that showed poor correlation or had unreasonable core analysis values were not used in the training data set. A final permeability log for each well was then computed using this trained neural network workflow. The permeability property was populated into the 3-D structural model using SGS and cokriged with the effective porosity property (Figure 17).

Net-to-Gross

Three net-to-gross (NTG) logs were created.

- NTG1 = effective porosity$_{2.4}$ /total porosity
- NTG2 = shale volume < 50%, and effective porosity$_{2.6}$ >19.5%
- NTG3 = shale volume < 65%, and effective porosity$_{2.6}$ >18%

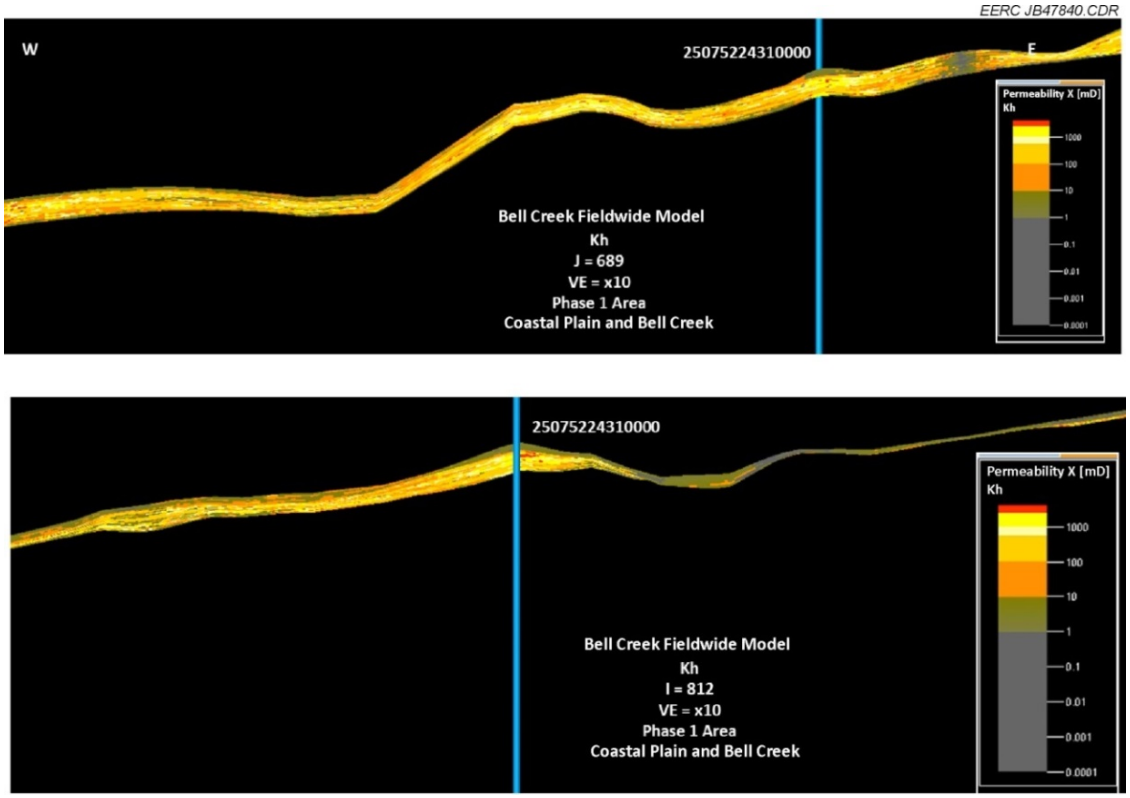

Figure 17. Phase 1 cross sections showing geostatistically populated horizontal permeability within the 3-D structural model. See Figure 9 for a map view of the sections; the 05-06 OW is shown.

NTG1 is simply the effective porosity property as calculated with the shale density equal to 2.4g/cm^3 divided by the total porosity property. This result in a ratio applied to each cell in the model, depending on the values found for both effective porosity and total porosity in each grid cell. NTG2 and NTG3 are calculated statements, thus creating a Boolean condition, so if the grid cell passes the statement conditions, then it is included in the net portion. If the grid cell does not pass the conditions, it is part of the gross portion only. NTG3 represented the best case as it correlated well with geologic interpretation and distribution shale filling the boundaries between phases in the Bell Creek oil field. Thus the NTG3 property was used in the dynamic modeling workflow.

Water Saturation

A J-function approach was used to create the water saturation reservoir property. The process was based on the core analysis data from 190 wells and 14 high-pressure mercury injection tests in the Muddy Formation in the Bell Creek oil field. The reservoir was divided into five flow units to better reflect the actual water saturation and any trends. A J-function for each flow zone was applied. A flow unit represents a basic element in the reservoir within which the rock has similar flow properties (Amaefule and Mehmet, 1993). The key factor in the determination of flow unit is the pore structure which is defined by rock mineralogy, texture, and macro sedimentary features (bedding, laminations, etc.). Many researchers have contributed to the understanding of flow units and further developed them as a reservoir characterization tool. According to flow unit determination, the reservoir is divided into five units:

- Excellent-quality reservoir (EQR)
- Good-quality reservoir (GQR)
- Medium-quality reservoir (MQR)
- Low-quality reservoir (LQR)
- Very low quality reservoir (VLQR)

In Figure 18, all core sample scatters are cross-plotted in one panel, and the flow zones are presented with different colors. This J-function approach with flow units was used to build the water saturation property within the 3-D structural model (Figure 19).

Uncertainty Analysis

Using an uncertainty analysis workflow, 127 realizations were calculated to analyze the following variables: NTG, effective porosity, oil–water contact, and water saturation. The results were then ranked according to STOOIP (stock tank original oil in place), and P10, P50, and P90 cases were selected for comparison against the base case model (Figure 20). All four model realizations were passed on for dynamic simulation; however, only the base case has been history-matched at this time.

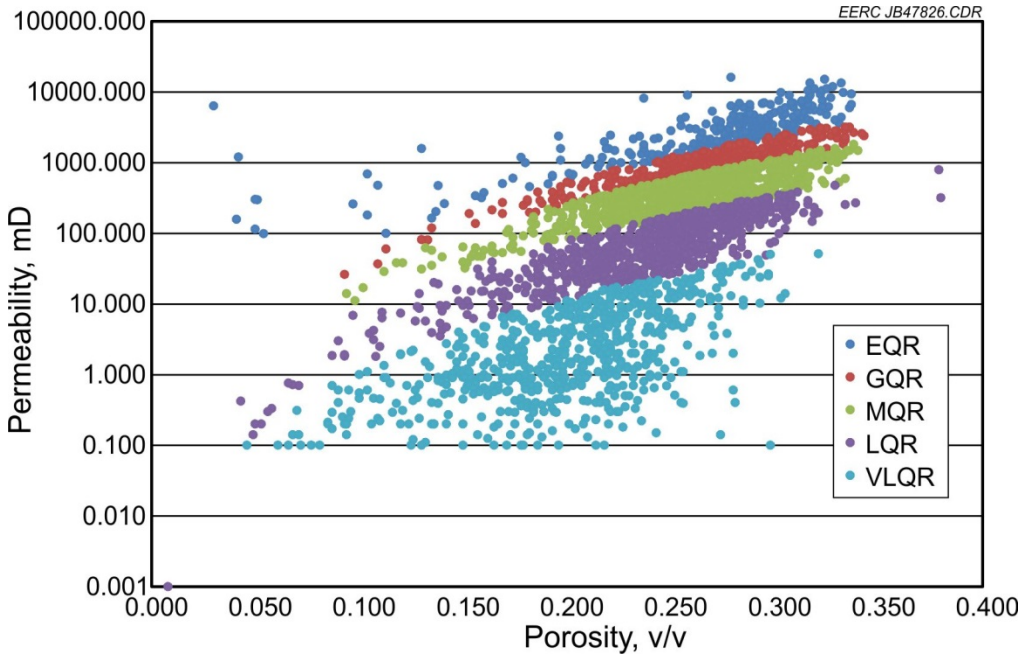

Figure 18. Permeability and porosity crossplot showing the correlation for all five flow units.

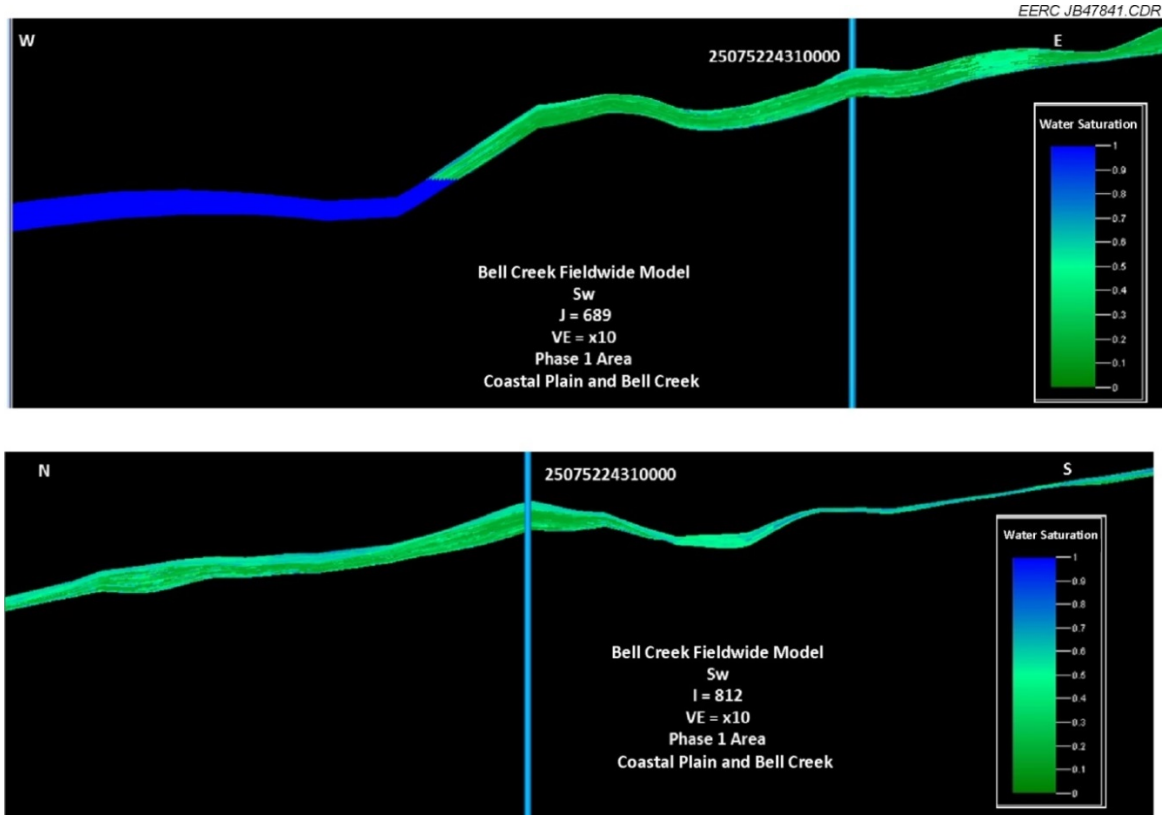

Figure 19. Phase 1 cross sections showing geostatistically populated water saturation property within the 3-D structural model. See Figure 9 for a map view of the sections; the 05-06 OW is shown.

EERC JB47848.CDR

Zones	Base Case Simulation Model STOIIP (in oil) [*10^6 STB]	Base Case Uncertainty Model STOIIP (in oil) [*10^6 STB]	P10 Case 121 STOIIP (in oil) [*10^6 STB]	P50 Case 65 STOIIP (in oil) [*10^6 STB]	P90 Case 38 STOIIP (in oil) [*10^6 STB]
CP	24	24	22	25	28
BC	366	362	339	363	385
Boundaries					
BCFieldBoundary	388	384	359	385	410
Phase 1	46	45	42	45	48
Phase 2	31	31	29	31	33
Phase 3	38	36	35	38	38
Phase 4	26	26	24	26	28
Phase 5	60	60	56	60	64
Phase 6	46	46	42	45	48
Phase 7	23	23	21	23	25
Phase 8	58	57	53	57	62
Phase 9	59	59	55	60	64

Figure 20. Comparison of the five models that represent the Version 2 effort of building a 3-D static model for the Bell Creek reservoir. The base case simulation model represents the values after an upscaling process has occurred on the base case uncertainty model. The P10 case is a pessimistic realization, underestimating the STOOIP during realization ranking. The P50 case represents an idealized base case for STOOIP based on the realization ranking. The P90 case is an optimistic realization, overestimating STOOIP during realization ranking.

Conclusions

After the Version 1 static model of the Phase 1 area was completed, Version 2 was built to represent a 200-sq-mile study area centered on the Bell Creek oil field. Version 2 consisted of 748 wells, six stratigraphically correlated zones, five petrophysical facies, and six reservoir properties conditioned to facies. An uncertainty analysis was also performed to obtain P10, P50, and P90 cases for dynamic simulation. A more robust workflow was used in Version 2 as compared to Version 1. All petrophysics were determined from well logs and core data in Techlog for Version 2, while Version 1 relied on precomputed petrophysics from a previous study (Encore Acquisition Company, 2009).

Limitations

Although the workflow was more robust in Version 2, a planned Version 3 model will aim at reducing the uncertainty even further by incorporating petrographics, outcrop field work, VSP (vertical seismic profile) surveys, 3-D seismic survey, base case pulsed-neutron logs, and additional core data. The petrophysical facies were correlated to core descriptions but not to petrographic descriptions. Outcrop fieldwork helps to provide a better stratigraphic and structure framework as well as explain the geologic history and depositional environments. The VSP and 3-D seismic surveys will provide a detailed structural framework with geobody representation and

values for reservoir properties that will be cokriged to the existing petrophysically derived properties.

Future Work

Upon completion of the following characterization activities, a Version 3 geologic model will be constructed:

- 35 base case pulsed-neutron logs interpreted
- 3-D seismic survey interpreted
- Two 3-D VSP surveys interpreted
- Core petrographic analysis interpreted, including the definition of depositional facies
- Additional core from two newly drilled wells characterized and interpreted

The base case pulsed-neutron logs will provide updated oil saturation, water saturation, and porosity. Both the 3-D surface seismic and 3-D VSP surveys will help to better define the structural framework, geobody characterization, and reservoir properties through the inversion process. Core petrographics will provide an insight into depositional facies and their relationship to petrophysically derived facies used in the Version 2 model. The additional, newly acquired core will be used to improve reservoir properties, especially some of the shale facies between phases.

PHASE 1 RESERVOIR SIMULATION

While the geologic model provides a framework for dynamic simulation activities, the dynamic reservoir model incorporates a variety of additional reservoir data to accurately simulate the reservoir's pressure and fluid mobilization response to injection or production processes. Much of the geologic and structural reservoir properties were directly incorporated through the integration of the 3-D geologic model. Several realizations of the static geologic model were generated using Schlumberger's Petrel® software. The static geologic model realizations having the mean OOIP value were exported to the Computer Modelling Group (CMG) Builder software (Computer Modelling Group, 2011) to construct a reservoir simulation model. The pressure, volume, and temperature (PVT) data, relative permeability data, and well production and injection history were brought into CMG Builder to begin the process of building the dynamic reservoir model.

Fluid flow simulation was performed on the dynamic reservoir model using CMG's General Equation of State Modeling (GEM) package. These flow simulation studies allowed the validation of the geologic model and the fine tuning of model parameters to match reservoir production, pressure, and injection responses through history matching. After a history match was performed, the predictive simulations with continuous CO_2 and CO_2/water alternating gas (WAG) injections were run.

Boundary

The dynamic reservoir model used for history matching and predictive simulations covers the Phase 1 area and a small portion of the surrounding areas, which was clipped from the fieldwide geologic model. Figure 21 displays a map showing the geologic model boundary (orange), the dynamic model boundary (red), and their relationship to the planned Bell Creek project development phases.

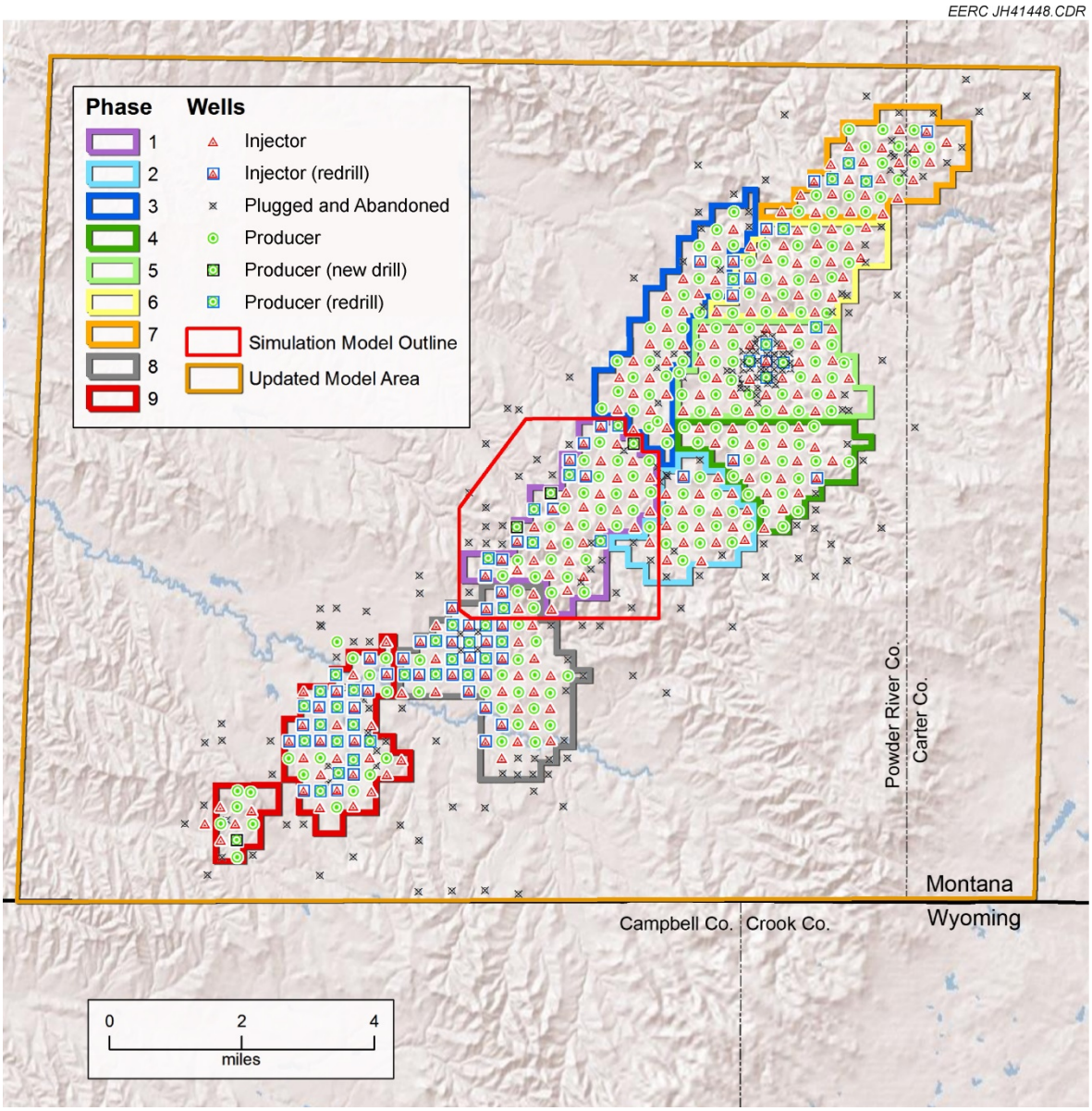

Figure 21. Map showing the geologic model boundary (orange), the dynamic model boundary (red), and their relation to the planned Bell Creek project development phases.

Gridding

The layering of different zones in the geologic model is shown in Table 3. Thirty-nine layers were incorporated into the geologic model, including six layers in the Coastal Plain zone and 20 layers in the Bell Creek sand zone. The horizontal cell size of the fieldwide geologic model is 50 ft × 50 ft. In all, the clipped 3-D geologic model has 3,906,630 cells (315 × 318 × 39), which presented a large computational workload for the compositional flow simulation. In order to reduce the computational burden in the process of reservoir simulation without impairing the geologic characteristics, upscaling of the fine geologic model was carried out by increasing the cell size to 100 ft ×100 ft and by reducing the layers of the Coastal Plain to one layer. After upscaling, the total number of cells was 973,557 (157 × 158 × 34). The final simulation model, which only includes Coastal Plain and Bell Creek zones, has 520,926 cells (157 × 158 × 21).

PVT Modeling

Simulator and Equations of State

PVT data for crude oil samples from the Bell Creek field were used to define PVT relationships under reservoir conditions. Constant composition expansion (CCE), differential liberation (DL) analysis, separator, swelling test, and fluid compositional analysis data were also available for oil samples. The Peng–Robinson (PR) EOS model was developed and tuned based on the available experimental PVT data using WinProp™ (Computer Modelling Group, 2011), a phase property program developed by CMG. CMG WinProp uses cubic EOS to perform phase equilibrium and property calculations.

The model contained seven components after grouping, which includes CO_2, N_2 to C_2H, C_3H to NC_4, IC_5 to C7, C8 to C13, C14 to C24, and C25 to C36. The EOS model is "tuned" to match laboratory data using nonlinear regression. Based on a general rule for selecting regression variables to exclude any EOS parameter that, by inspection, cannot significantly affect the calculated value of any of the regression data, main parameters include the lightest/heaviest binary interaction coefficient, Ω_a and Ω_b for the lightest fraction and the heaviest fraction in the regression process. The model showed less than a 5% variance between experimental data and calculated results of the EOS after tuning. Comparative results between the EOS tuned simulation results and the PVT experimental data are presented in Figures A-1 through A-4 in Appendix A.

Table 3. Upscaling of Geologic Model to the Dynamic Simulation Model

	Number of Layers	
Zone	Original	After Upscaling
Shell Creek Shale	3	0
Springen Ranch Member	4	0
Coastal Plain	6	1
Bell Creek Sand	20	20
Rozet Member	3	0
Skull Creek Shale	3	0

Minimum Miscibility Pressure

CO_2 EOR operations are most effectively implemented when operating above the minimum miscibility pressure (MMP). As such, it is essential that the original oil makeup and properties are

well understood, as well as the oil properties and makeup after decades of primary and secondary recovery. As oil is produced under primary and secondary recovery, many of the light-end components are preferentially produced, changing the overall composition of the original crude. These changes can result in a shift in the pressure it takes for CO_2 and the reservoir crude oil to become miscible. To better understand this potential shift in the MMP, laboratory-derived slim-tube experiments were run on both the recombined original formation oil (GOR [gas-to-oil ratio] of 275 scf/bbl) and a recombined current formation oil (GOR of 40 scf/bbl). The resulting MMP values were 3181 psia for the original formation oil and approximately 1400 psia for the current formation oil (Figure 22).

The tuned EOS was then used to predict the MMP utilizing the original formation oil composition and pure CO_2 and resulted in a MMP of 2970 psia. The EOS was then numerically flashed to a GOR of 40 scf/bbl. Predictions were then run on the flashed oil and pure CO_2 and resulted in a predicted MMP of 1180 psia (Figures 23 and 24 and Table 4). It was then deemed that this EOS would be adequate for handling the behavior of the formation oil from the history-matching process of primary and secondary recovery and still be valid for predictions of the CO_2 EOR processes.

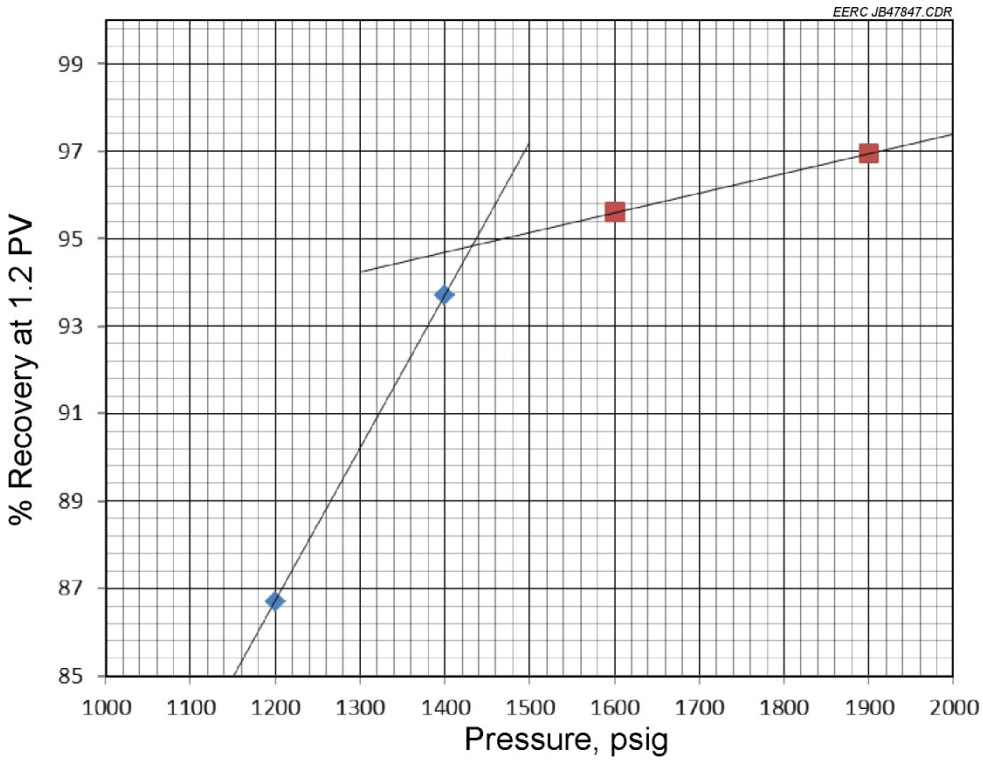

Figure 22. Slim-tube MMP from Core Laboratories with a GOR of 40 scf/bbl.

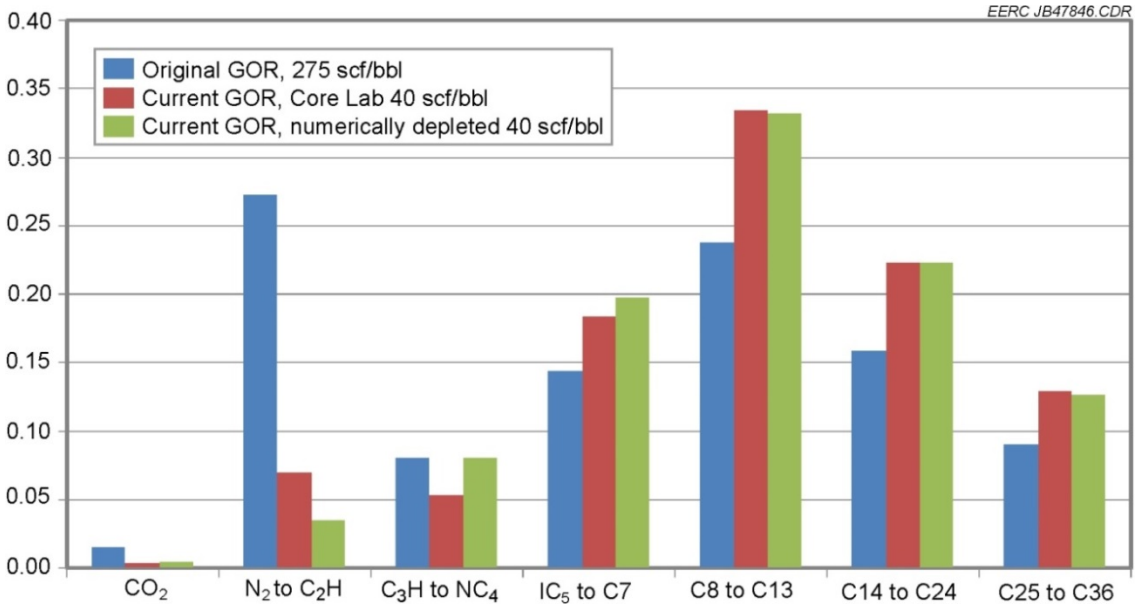

Figure 23. Composition comparison of original oil, Core Laboratories residual oil, and numerically depleted oil.

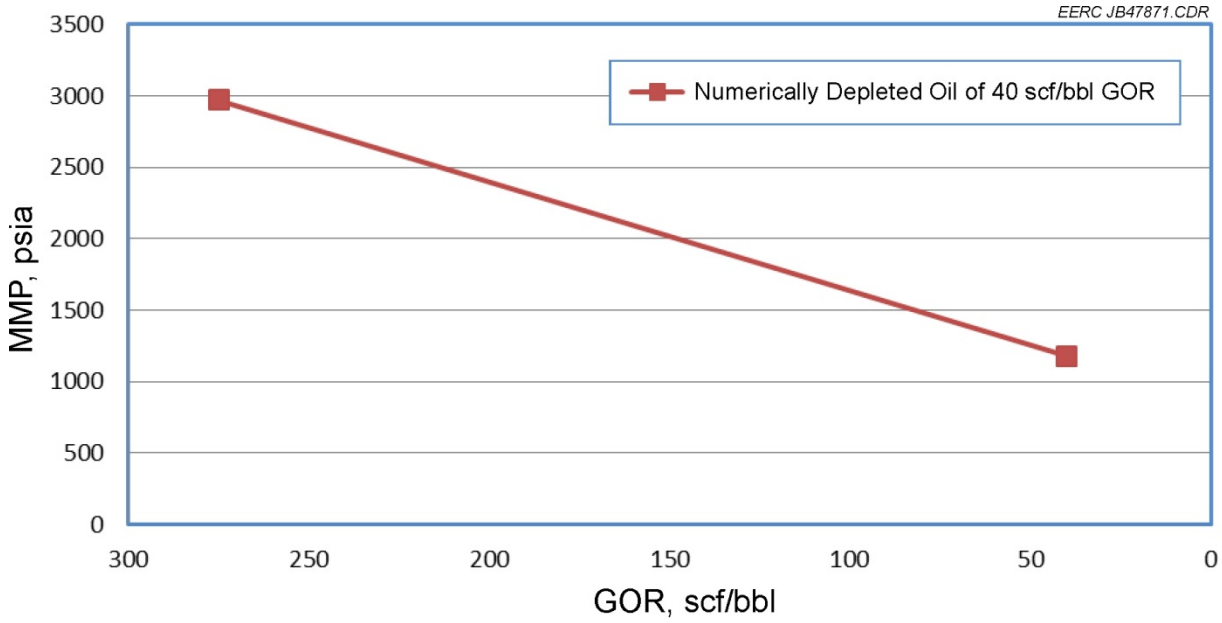

Figure 24. MMP comparisons of original oil and numerically depleted oil with a GOR of 40 scf/bbl.

Table 4. Composition Comparison of Original Oil, Core Laboratories Residual Oil, and Numerically Depleted Oil

Pseudo-components	Fully Saturated Mol Frac, lab-recombined	40 scf/bbl GOR Mol Frac, lab-recombined	40 scf/bbl GOR Mol Frac, numerically depleted
CO_2	0.0158	0.0042	0.0046
N_2 to C_2H	0.2726	0.0704	0.0352
C_3H to NC_4	0.0803	0.0539	0.0807
IC_5 to C7	0.1444	0.1846	0.1973
C8 to C13	0.2375	0.3347	0.3327
C14 to C24	0.1592	0.2229	0.2232
C25 to C36	0.0901	0.1292	0.1263

History Matching

History matching is a method of adjusting reservoir characteristics (variables) within a simulation model to match historical field data (production or injection data) through an iterative trial-and-error process. This trial-and-error process varies parameters and properties within accepted and realistic engineering and geologic limits. In this way, the resulting properties and parameters still accurately reflect the original "hard" data. History matching reduces the geologic uncertainties, which will allow for more accurate prediction of future reservoir performance both during and after injection. Simulations aiming at matching the reservoir's oil and water production during primary depletion and waterflooding were run using the dynamic reservoir model described in the previous sections. The history matching was performed using CMG's CMOST and GEM software packages.

One hundred nine vertical wells were included in the simulation model: 72 production wells, 36 injection wells (35 were converted to injectors from producers), and one monitoring well. The grid was 157 × 158 × 21 with 520,926 total cells in the dynamic model. The grid block size was 100 ft in length and 100 ft in width. The thickness of each grid block varied, with an average grid cell thickness of 1 ft. Figure 25 shows a plan view of permeability in the Bell Creek sand, the locations of the injection and production wells, and the outline of the Phase 1 area.

The history match was performed utilizing production and injection rates from the field spanning from 1967 to 2013. The reason behind simulating the full history was to provide an estimate of fluid saturation and reservoir pressure before the CO_2 flood and to provide an accurate representation of current reservoir conditions. During the history-matched period, liquid production rates were used as primary constraints, and bottomhole pressures were used as secondary constraints. Historic oil production, water production rates, and water cut of each well were used to compare with the simulations. After a number of simulation runs which included modifications of the relative permeability curve, permeability, and well productivity indices, a reasonably good match of the production history was obtained, as shown in detailed simulation results presented in Appendix B.

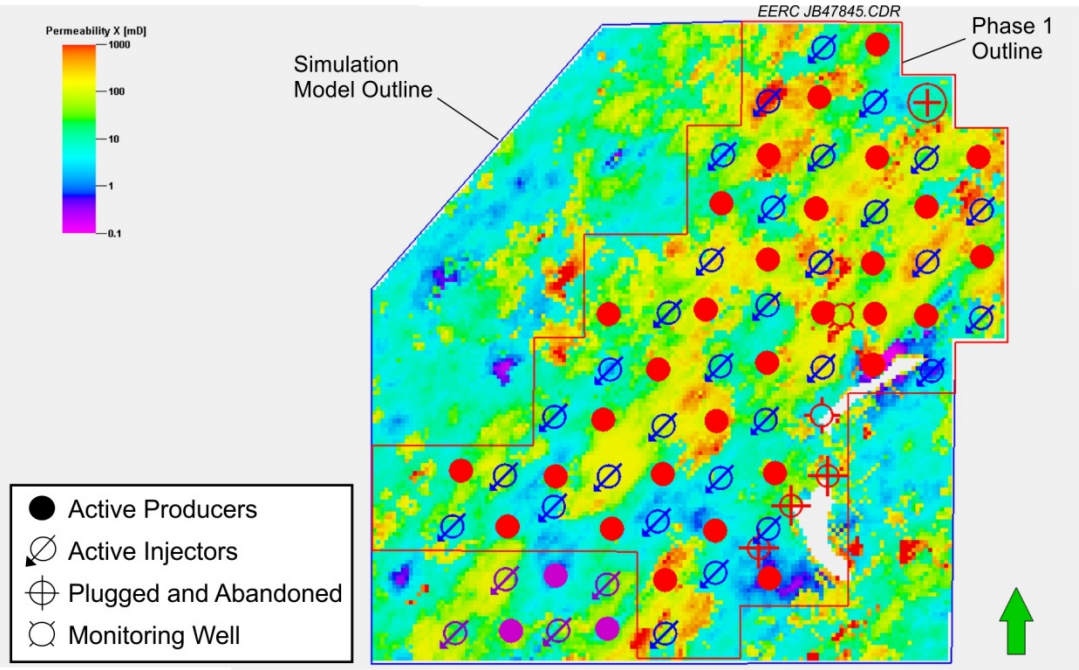

Figure 25. Plan view of Bell Creek sand permeability in the Phase 1 area.

Phase 1 Areawide History-Matching Results

The detailed history-matching results of the Phase 1 areawide dynamic reservoir model are provided in Appendix B (Figures B-2–B-8) and are briefly discussed here.

After 130 history-matching runs, a relatively close match was achieved between the observed oil rates, water cut, gas rate, and the simulated results (Figures 26–28). Initial hydrocarbon production at the Bell Creek oil field was produced by solution gas drive, so the gas rate initially increased rapidly and then dropped during the primary depletion.

The actual reservoir pressure history, except for some initial reservoir pressure data (1100–1200 psi at an average depth of 4500 ft) obtained in drillstem tests (DSTs) and recent data from testing within the last 3 years, is unavailable; hence, the simulated reservoir pressure response could not be verified during much of the history (Figure 29). The history-matching results show that the reservoir model was able to closely match the injected and produced volumes and water cut very well.

Individual Well History-Matching Results

In order to verify the primary history-matching model, individual wells were also history-matched. The detailed results are provided in Appendix B (Figures B-9 through B-14). These results show the water-cut behavior observed in primary and secondary recovery for 18 individual wells, which are in good agreement. The simulated oil rates of these individual wells also match the actual oil rates well. The model was able to produce the specified liquid rates throughout the history. As a result, liquid rates of individual wells are not shown in the history-matching plots.

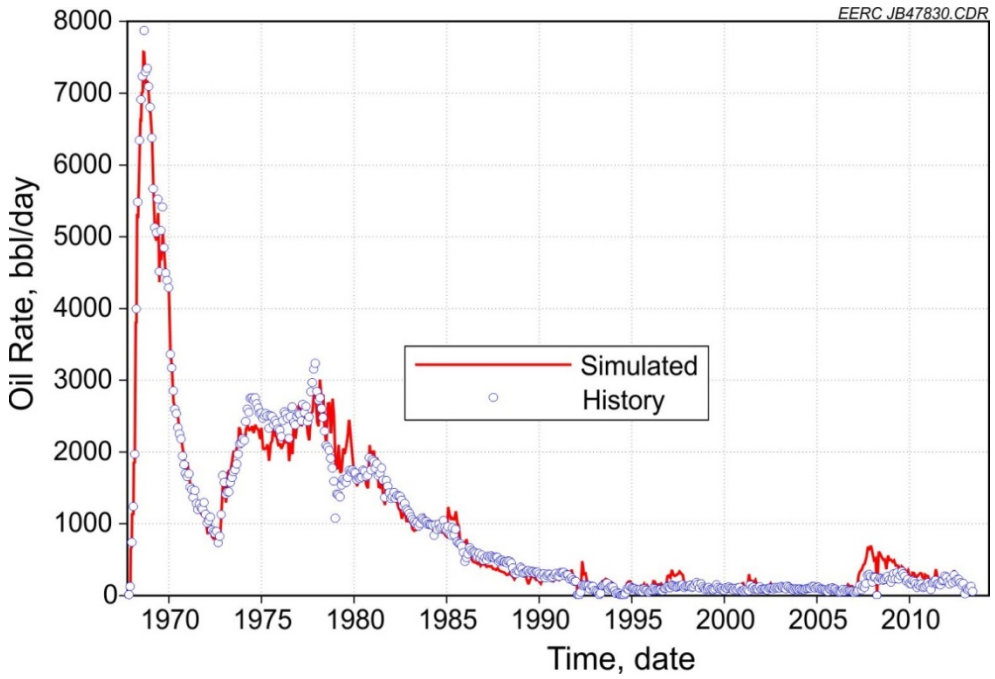

Figure 26. History-matching result of field oil rate, where the circles represent the field data and the solid line represents the simulation results.

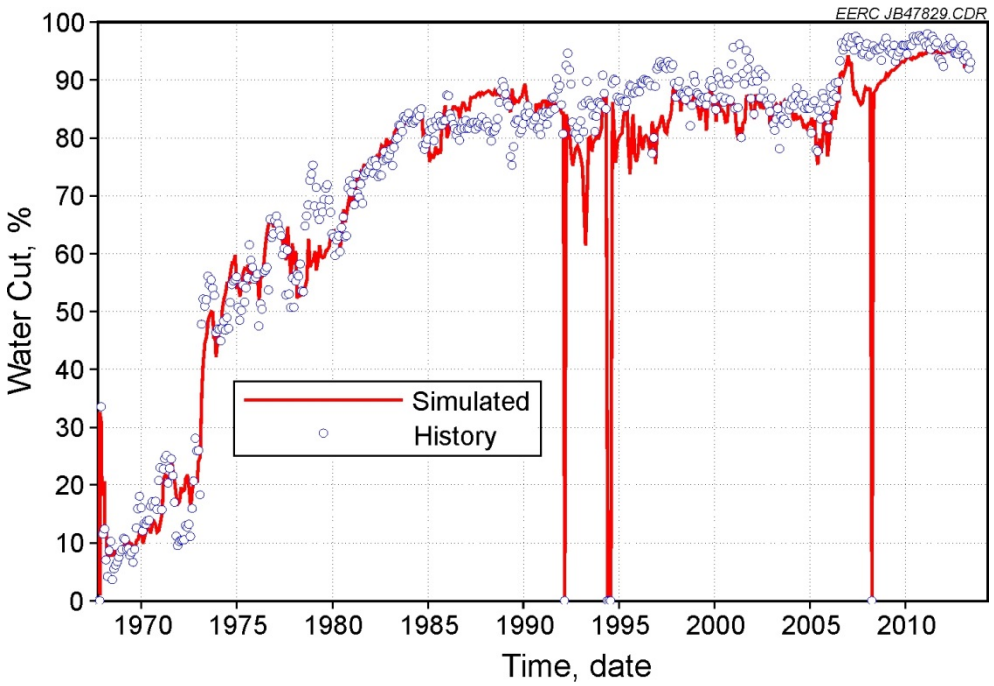

Figure 27. The history-matched results of simulated and actual water cut of the field are shown, where the circles represent the field data and the solid line represents the simulation results.

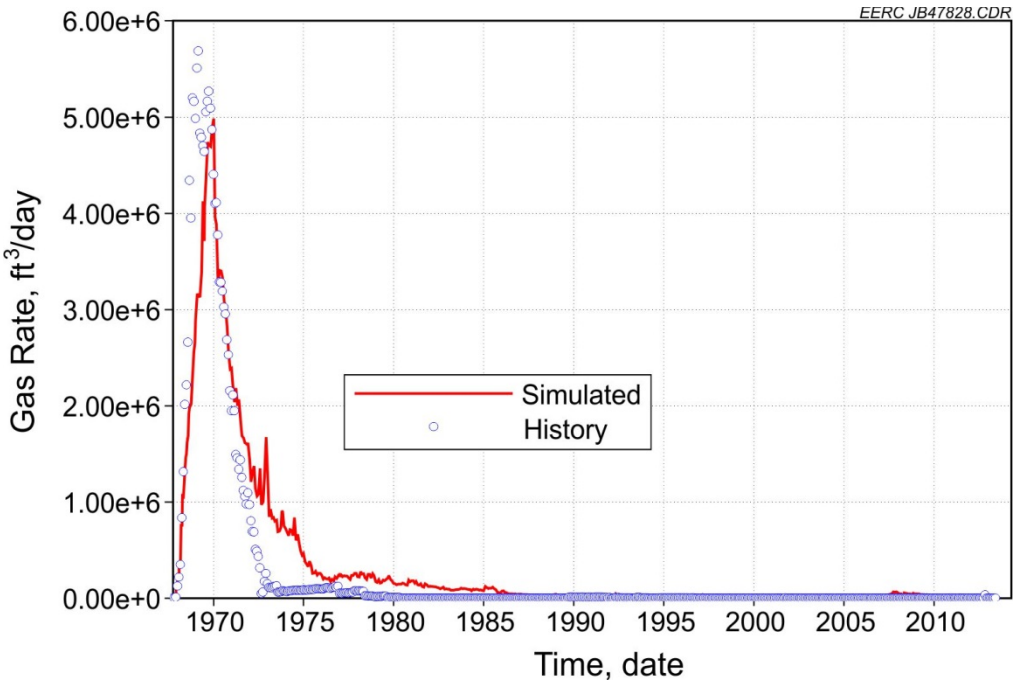

Figure 28. History-matching result of field gas production rate, where the circles represent the field data and the solid line represents the simulation results.

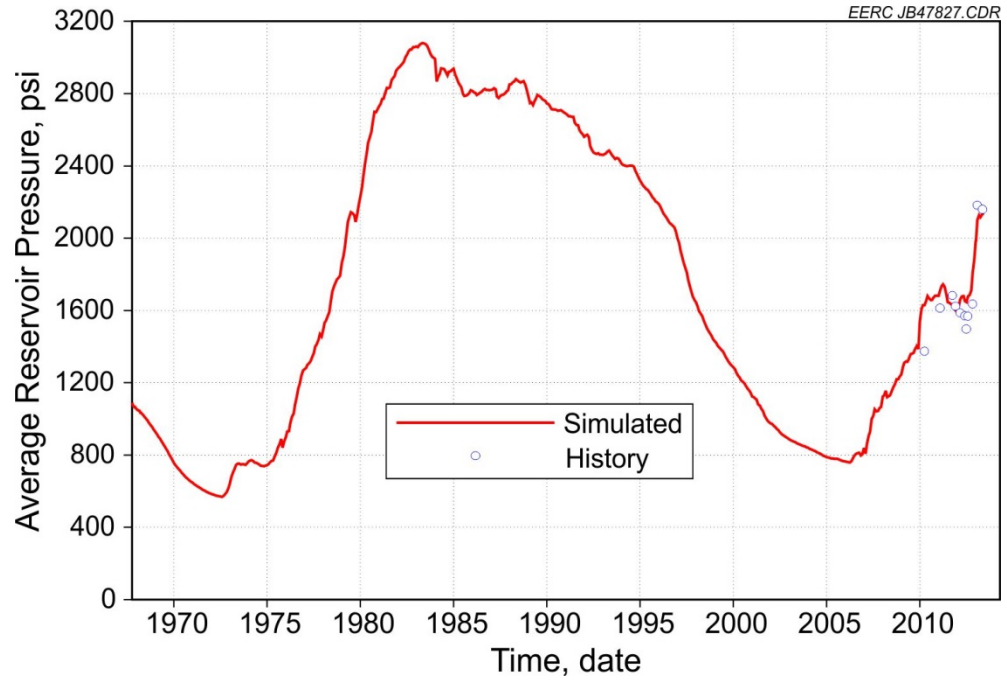

Figure 29. Average reservoir pressure over the reservoir's history, where the circles represent the field data and the solid line represents the simulation results.

Predictive Fluid Flow Simulations

Once a satisfactory history match was obtained, predictive simulations were performed to evaluate the effects of various CO_2 injection schemes on movement of injected CO_2 in the reservoir over time. Although the performance of the waterflooding program in the Bell Creek oil field had been successful (37.7% primary + secondary recovery), it still left an estimated 221 million barrels behind in the reservoir. This has prompted engineering studies to investigate means of economically recovering additional incremental oil production. Continuous miscible CO_2 flooding and CO_2 WAG were chosen as potential tertiary EOR processes, and both were used to evaluate various future production and injection scenarios in the predictive simulations reported here.

Predictive simulations were repeated under different operating scenarios to evaluate the reservoir performance. In order to provide the comparison of the CO_2 movement and long-term CO_2 fate, predictive simulations were performed using the Phase 1 model, as described above. During the prediction stage, the matched parameters were used to evaluate the movement of CO_2 and CO_2 breakthrough times at monitoring and production wells.

According to the CO_2 injection plan, a total of 26 active injection wells and 26 active production wells are included in the predictive simulation model. The CO_2 injection rate was specified to be 50 MMscf/day. In all cases, a minimum bottomhole flowing pressure was specified for the production wells as the operating constraint. The CO_2 injection wells were controlled by CO_2 injection rates and limited by maximum bottomhole pressure constraints.

Phase 1 Area Simulation Model

Continuous CO_2 injection and WAG (1:1 injection ratio) processes were simulated for the Phase 1 model to evaluate their effect on CO_2 EOR efficiencies, CO_2 breakthrough time at the monitoring well, various production wells, and long-term CO_2 plume and pressure behaviors. All of the history-matched properties were used to provide an input to a Phase 1 predictive simulation model for the CO_2 flood. In other words, the history match discussed in the previous section was used as the initial condition for the predictive simulation model to develop the reservoir monitoring strategies.

Six cases were run to investigate the effect of CO_2 injection on the EOR process using three hydrocarbon pore volumes (HCPVs) of injected fluids (Table 5). Simulation cases were performed to investigate and identify reservoir management factors regarding 1) injection pressure, 2) WAG cycle length, and 3) injection mode (WAG or continuous injection).

Discussion of Results

The simulation results for the Phase 1 area model are provided in Appendix B (Figures B-16–B-66) and are summarized in Tables 6 and 7.

Table 5. Simulation Parameters for Each Investigatory Case

Case	Total Volume Injected, HCPV	CO_2 Injected, HCPV	Flood Style	Injector Pressure, psi	Producer Pressure, psi	Cycle Length
1	3	1.5	WAG	2500	2300	3 month 1:1
2	3	1.5	WAG	2800	2300	3 month 1:1
3	3	1.5	WAG	2500	2300	2 month 1:1
4	3	1.5	WAG	2800	2300	2 month 1:1
5	3	3	Continuous CO_2	2500	2300	–
6	3	3	Continuous CO_2	2800	2300	–

Table 6. Results of Simulation for Produced and Injected Water and CO_2 Volumes (3 HCPVs)

Case	Cumulative Injected CO_2, Bscf	Cumulative Water Injection, million bbl	Cumulative Produced Gas, Bscf	Cumulative Water Production, million bbl	Stored CO_2, Bscf	Stored CO_2, million tons
1	107	11.0	77	16.9	30	1.72
2	167	33.9	137	35.6	30	1.75
3	103	11.6	74	17.2	29	1.67
4	166	34.3	136	36.0	30	1.76
5	329	–	270	14.9	59	3.28
6	356	–	296	15.2	60	3.35

Table 7. Results of Simulation for Produced Hydrocarbons and Flood Performance (3 HCPVs)

Case	Cumulative Oil Production, million bbl	Peak Oil Production Rate, bbl/day	Average Reservoir Pressure, psi	Recovery Factor, %	Net Utilization Factor, Mscf/bbl
1	4.13	1615	2448	14.36	7.37
2	7.61	3783	2614	26.46	3.99
3	4.10	1626	2447	14.25	7.20
4	7.65	3845	2606	26.52	3.96
5	5.43	1572	2377	18.85	10.85
6	5.55	2018	2374	19.27	10.84

Discussion of Incremental Oil Recovery, Utilization Factor, and Oil Production

The incremental oil recoveries versus time and versus HCPVI of six CO_2 injection cases are shown in Figures 30 and 31, respectively. Among the six prediction scenarios, the WAG processes with operating injection pressure of 2800 psi, namely, Cases 2 and 4, yield the highest oil recovery. The oil recoveries of WAG Cases 1 and 3 with operating injection pressure of 2500 psi are much lower mainly due to the injectivity issue resulting from the lower injection pressure constraint. The oil recovery increase of continuous CO_2 injection, Cases 5 and 6, are similar.

The CO_2 utilization factors of Cases 1 through 6 are shown in Table 7. WAG processes (Cases 1 through 4) have CO_2 utilization factors of 3.96 or 7.20 Mscf/bbl for various operating injection pressures, while the continuous CO_2 injection gave high CO_2 utilization factors of 10.85 Mscf/bbl.

The daily oil production rate of each case is shown in Figure B-20, and the peak oil rates of the six cases are listed in Table 7. The cumulative oil production rates of six cases are shown in Figure B-21 and Table 7. The peak oil rates of WAG processes with injection pressure of 2800 psi (Cases 2 and 4) are twice the peak oil rates of the other four cases. The cumulative oil production rate of WAG processes, Cases 2 and 4, are much higher than the other cases.

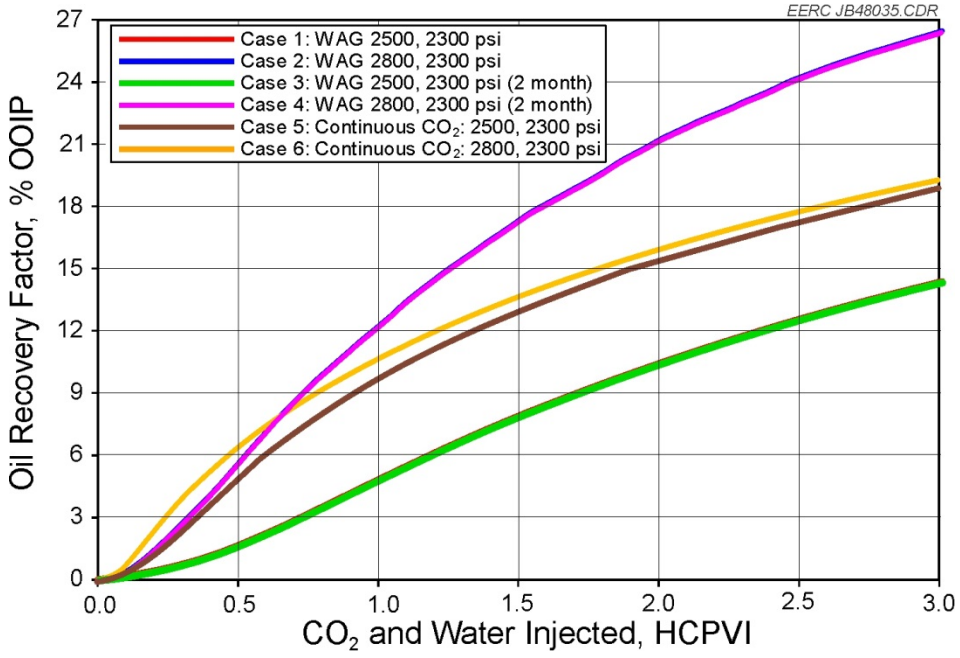

Figure 30. Incremental oil recovery vs. time of Cases 1 through 6.

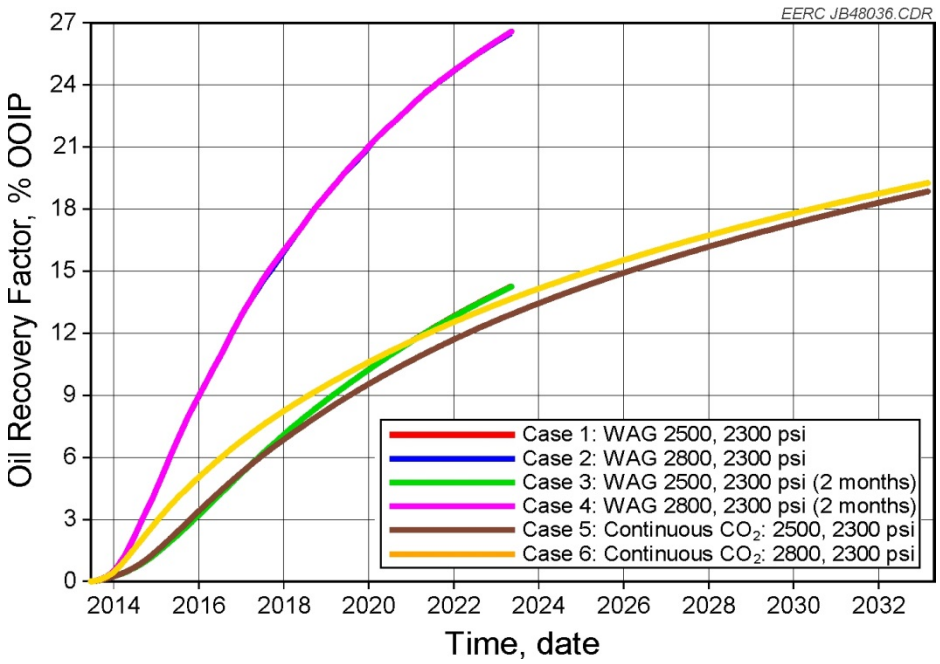

Figure 31. Incremental oil recovery vs. HCPVI of Cases 1 through 6.

Effect of Injection Pressure

The injection pressure constraints of 2500 and 2800 psi for injection wells were used in the predictive simulation cases (Table 5). The injection profiles of CO_2 and water are shown in Figure B-16–B-19. The predictive results show that the injection pressure significantly affects the actual amount of CO_2 injected, and cases with injection pressures of 2500 psi experienced injectivity issues. The Phase 1 injection rate of CO_2 was set at 50 million standard cubic feet (MMscf)/day, and water was injected at 20,125 bbl/day. This rate was unable to be met in lower pressure WAG simulations (Cases 1 and 3) because of numerical pressure constraints, with only 60% of CO_2 and 15% of water being injected in Case 1. At higher injection pressures (Cases 2 and 4), flow rates were achieved and did not significantly limit CO_2 injectivity, and water injectivity increased to 46% of the desired volume. A 57% increase in peak oil production rate was observed when injection well pressure was increased from 2500 to 2800 psi (Cases 1 and 2); however, this increase in pressure also results in higher rates of produced gas.

With regard to the net CO_2 utilization factors, WAG Cases 2 and 4 (operating pressure 2800 psi) have net CO_2 utilization factors of around 3.9 Mscf/bbl, and the net CO_2 utilization factors of WAG Cases 1 and 3 (operating pressure 2500 psi) was 7.2 Mscf/bbl. The net CO_2 utilization factor of the continuous CO_2 injection, Cases 5 and 6, was 10.8 Mscf/bbl.

Effect of WAG Cycle Length

The effect of varying the WAG cycle length (3 or 2 months) was minimal and had virtually no effect on results (Table 5). With the other injection parameters held the same, the predictive simulation results of different cycle lengths are virtually identical for Cases 1–4, indicating the

WAG cycle lengths of 3 and 2 months did not affect the oil recovery in these cases. Changing the flood style to direct CO_2 injection, however, reduced peak oil production slightly (3%) at low pressures and more drastically (47%) at higher pressures. Varying the pressure led to higher peak oil and enabled injection of the desired rates of CO_2; higher rates of water injection, however, also resulted in faster breakthrough. Altering the cycle rate did not significantly alter the simulation results.

Effect of Injection Mode

In order to optimize the CO_2 flood design, the predictive simulation of continuous CO_2 injection and 1:1 WAG processes was performed to assess the efficiency of each method on injectivity into the Bell Creek reservoir. WAG simulations were performed using 1.5 HCPVs of CO_2 and 1.5 HCPVs of water, whereas continuous CO_2 injections injected 3 HCPVs of CO_2. For the continuous CO_2 injection process, the daily CO_2 injection rate was 50 MMscfd, which was distributed to 26 injection wells. For the WAG processes, the daily CO_2 injection rate was also 50 MMscfd, which was distributed to 13 injection wells, and the daily water injection rate of 20,125 bbl was divided and distributed to the other 13 injection wells. To evaluate the effectiveness of the injection mode, the results of Case 2 (best WAG case) and Case 6 (best continuous injection case) were compared. The incremental oil recovery of Case 2 (WAG) is 26.46% OOIP after 3 HCPVI, while the oil recovery is 19.27% OOIP for Case 6 (Table 7, Figures 30 through 31). Besides a higher peak oil rate, Case 2 also shows an overall higher oil rate and faster recovery rate than that of Case 6 (Figure B-20).

CO_2 Stored

While the mass of stored CO_2 within the reservoir was not strongly affected by WAG cycle length, changing the method to direct injection nearly doubled CO_2 storage, although twice as much CO_2 was injected. The stored CO_2 for the WAG processes was about 1.7 million tons after 3 HCPV injection, while the stored CO_2 for the continuous CO_2 injection processes was about 3.3 million tons. This discrepancy is caused by doubling the volume of cumulative CO_2 injected for the continuous CO_2 injection cases compared to the WAG cases. The results of each injection case, which illustrate the amount of CO_2 injected versus the amount of CO_2 that is incidentally stored, are shown in Figure 32 and Figures B-31–B-36.

CO_2 Plume Extent and Breakthrough Time

The CO_2 plume maps of Cases 1–6 at 1, 2, and 3 HCPVI are shown in Figures B-37–B-42, and the CO_2 plume maps of each case at 1 HCPVI are shown in Figures 33–38. The CO_2 plume maps show that with the progression of CO_2 injection (1 HCPVI–>3 HCPVI), the unswept areas in the Phase 1 decreased gradually, and the CO_2 plume increased steadily but was basically contained in the Phase 1 area, as illustrated by Figure 39 which shows how CO_2 progressed in Case 2 as more CO_2 was injected.

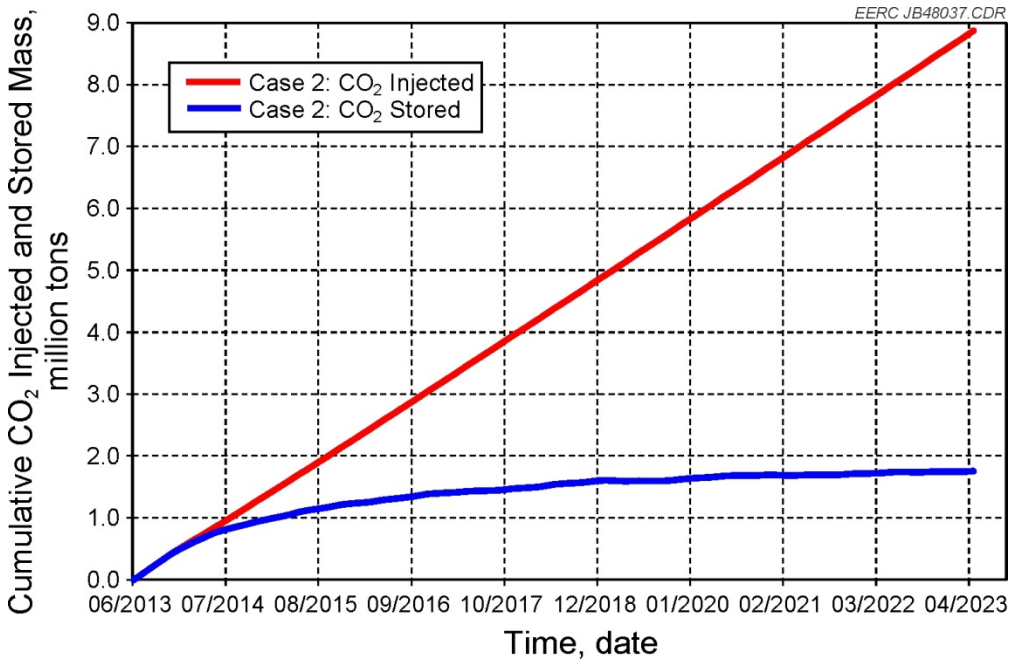

Figure 32. Case 2 cumulative CO_2 injected and stored.

The cross section between Wells 05-06, 05-06 OW and 05-07 are shown in Figures 40–45, which show the changes of CO_2 saturation/CO_2 movement of Case 2 at 1 month, 3 months, 6 months, 12 months, 18 months, and 24 months, respectively, after the start of CO_2 injection. Well 05-06 is the production well, 05-06 OW is the monitoring well, and 05-07 is the injection well. For Case 2, the first 5 months of CO_2 injection are continuous injection, followed by a 3-month WAG process. During the CO_2 injection process as shown in Figures 40–42, the saturation of CO_2 increased gradually, and more areas were swept by the injected CO_2. Then the WAG process started. Well 05-07 started injecting water as shown in Figures 43–45; CO_2 saturation around Well 05-07 decreased significantly; and the earlier injected CO_2 was pushed toward Production Well 05-06 by passing through Monitoring Well 05-06 OW. The earliest CO_2 breakthrough at Monitoring Well 05-06 OW was 5 to 6 months, depending on the case. The prediction scenarios with an operating pressure of 2800 psi have CO_2 breakthrough times at the first production well after 2 months, while the CO_2 breakthrough time for the cases with an operating injection pressure of 2500 psi was 3 months.

Conclusions

Based on the Version 1 3-D geologic model (2011), a number of efforts in the areas of flow units, water saturation, and permeability, etc., were made to improve the detailed geologic modeling culminating in a Version 2 model. A 3-D static geologic model of the Phase 1 area was clipped from the full-field geologic model (Version 2) and used as input to perform the dynamic simulations. The geologic model of the Phase 1 area was validated through history matching and then was used for various predictive CO_2 injection simulation scenarios.

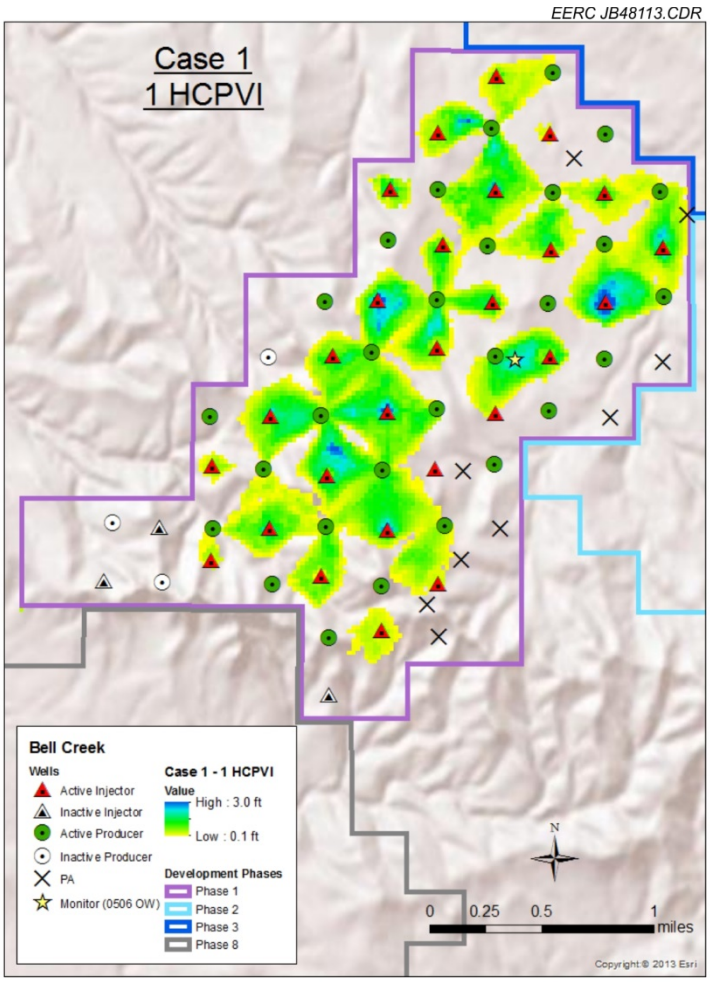

Figure 33. CO_2 plume for Case 1 (1 HCPV injected).

Key results of current simulation work include the following:

- Simulation of PVT tests on Bell Creek crude oil samples was performed by tuning a seven-component PR-EOS model. The simulated results of standard PVT tests match the laboratory measurements well. The composition of residual oil from the numerical liberation perfectly matched with the composition of the recombined oil used in the lab experiment. According to the PVT simulation, the MMP of the initial recombined oil was 2970 psia, and when this oil was numerically flashed to 40 GOR, it had an MMP of 1180 psia, closely matching current oil conditions and laboratory results.

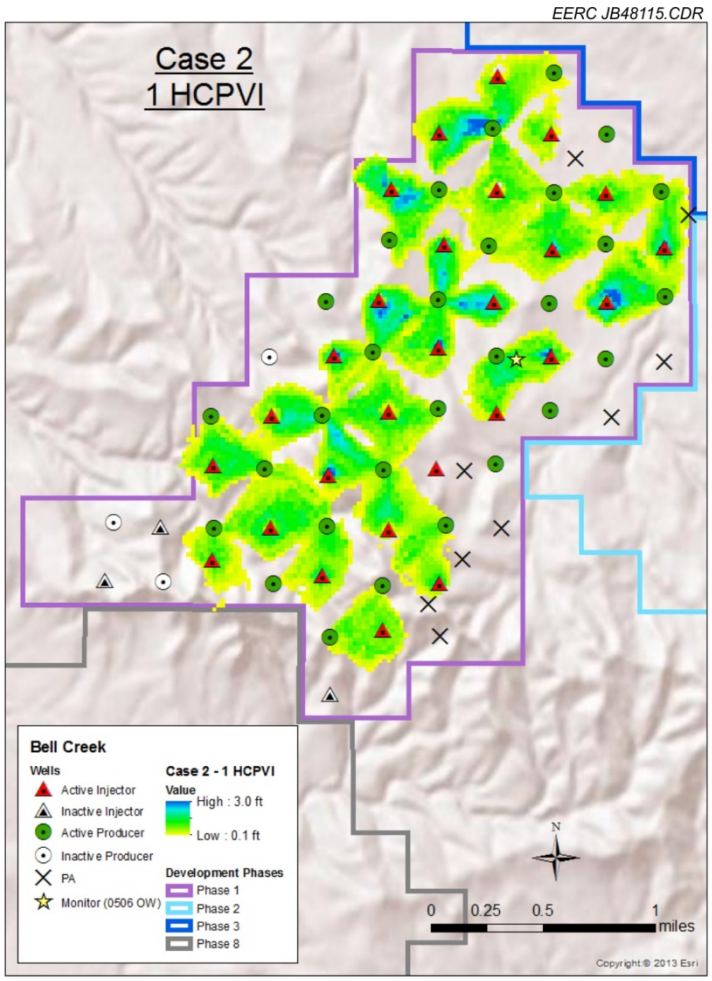

Figure 34. CO_2 plume for Case 2 (1 HCPV injected).

- The reservoir simulation model closely mimics the historical production behavior after 46 years of production and injection. A good history match was obtained for the Phase 1 compositional simulation model in terms of oil rate, liquid rate, water cut, and GOR. This matched model was then used for predictive simulations.

- The estimated incidental CO_2 storage capacity varied from 3.28 to 3.35 million tons of CO_2 from 3 HCPVs of continuous CO_2 injection. In the case of 3 HCPV WAG (1:1) injection (1.5 HCPV of CO_2), incidental CO_2 storage capacity varied from 1.67 to 1.75 million tons of CO_2.

- The predictive simulation results indicate that the WAG process yields a faster oil recovery and better sweep efficiency and may be more effective than the continuous CO_2 injection. The incremental oil recovery of WAG Case 2 is about 12%, 21%, and 26% for 1, 2, and 3 HCPVI, respectively, while the oil recovery of continuous CO_2 injection Case 6 is about 11%, 16%, and 19% for 1, 2, and 3 HCPVI, respectively.

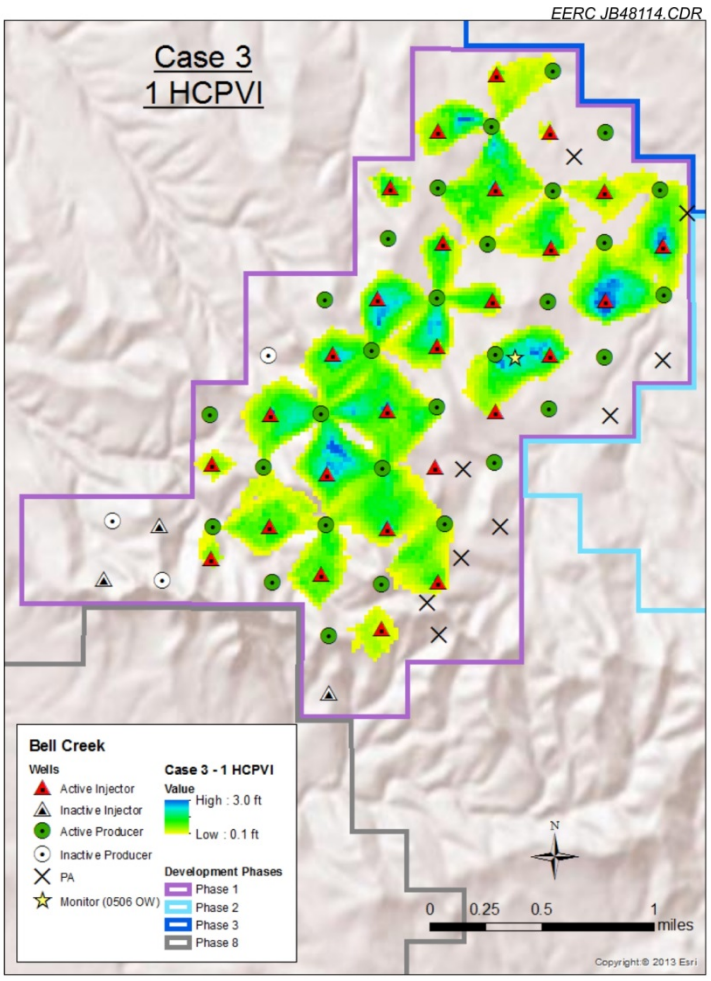

Figure 35. CO_2 plume for Case 3 (1 HCPV injected).

- As for the CO_2 breakthrough time, the earliest CO_2 breakthrough occurred 3 months after the start of CO_2 injection for the continuous CO_2 flooding scenario, while the earliest CO_2 breakthrough of the WAG scenario is 2 months. The simulation results also show that injected CO_2 is expected to reach the newly drilled monitoring well 6 months after injection begins for the continuous CO_2 flooding scenario and 5 months after injection begins in the WAG case.

- The CO_2 utilization factors of WAG processes was 3.9 Mcf/bbl for cases with injection pressure of 2800 psi and 7.2 Mcf/bbl for cases with injection pressure of 2500 psi, while the CO_2 utilization factors of continuous CO_2 injection is 10.8 Mcf/bbl after 3 HCPVI.

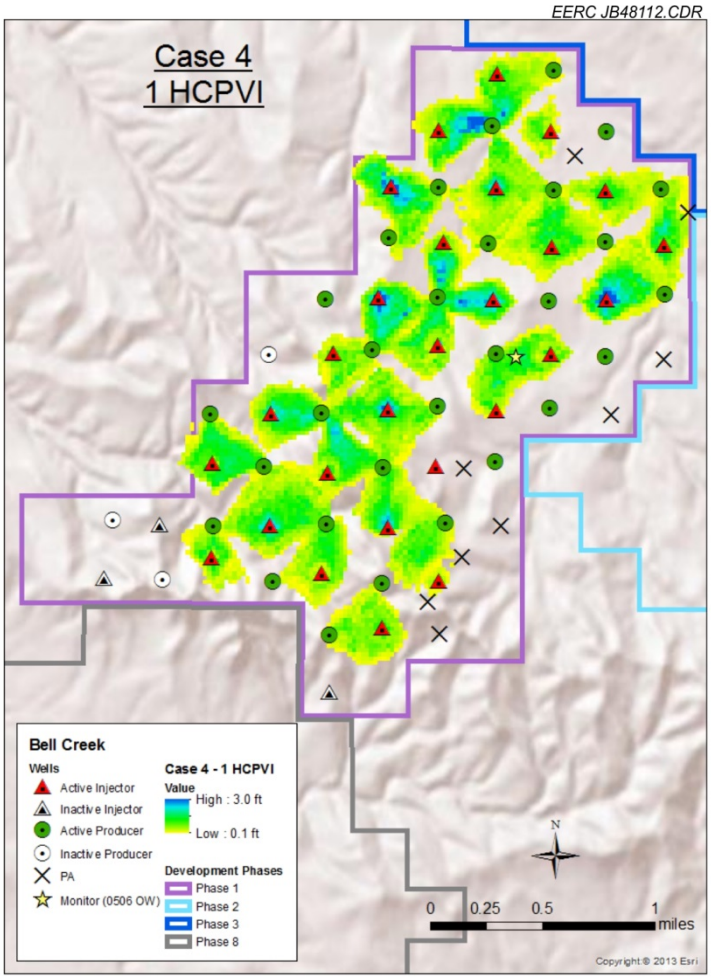

Figure 36. CO_2 plume for Case 4 (1 HCPV injected).

Limitations

Even though several years of reservoir pressure were matched, one of the limitations of this dynamic simulation work is still the history matching of average reservoir pressure, since only the initial reservoir pressure and the average pressure of years 2010–2013 are available. More historical reservoir pressure data would lead to more accurate calculated pressure; however, these data are not available.

The history-matching methods are also worthy of discussion. The manual history-matching method was used for this dynamic simulation through running simulations for historical period, comparing results to actual field data, and adjusting simulation input to improve match. The selection of adjusted input data is based on analysis, knowledge, and experience. This process is very onerous and time-consuming. The automatic history-matching techniques, e.g., aided by CMG's CMOST, automatically vary reservoir parameters until criteria are achieved and a history

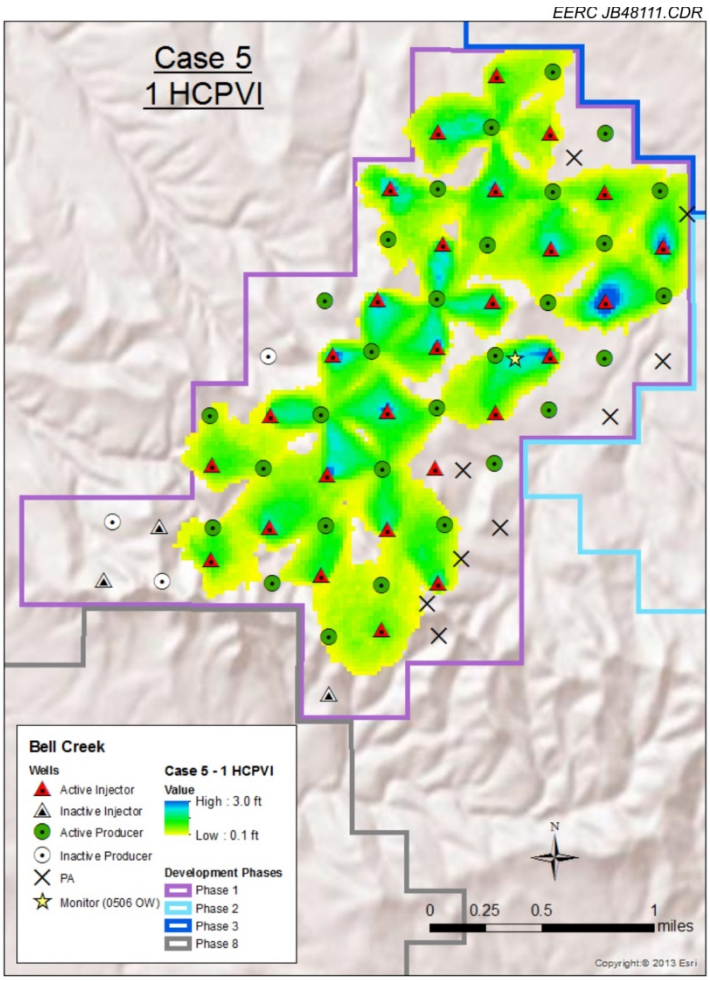

Figure 37. CO_2 plume for Case 5 (1 HCPV injected).

match of field performance is obtained. Computer-aided history matching by CMOST, which minimizes the global objective function error, e.g., the difference between observed reservoir performance and simulation results, is planned for the future round of dynamic simulations.

During the predictive simulation of CO_2 flooding, the relative permeability hysteresis and CO_2 solubility in the aqueous phase were not accounted for, so the estimated incidental CO_2 storage capacity values for different cases may appear to be on the lower side. The WAG ratio of 1:1 was used in all of the simulation cases, but in the near-future predictive simulation, injecting other ratios may be evaluated for their effects on incidental CO_2 storage and incremental oil recovery.

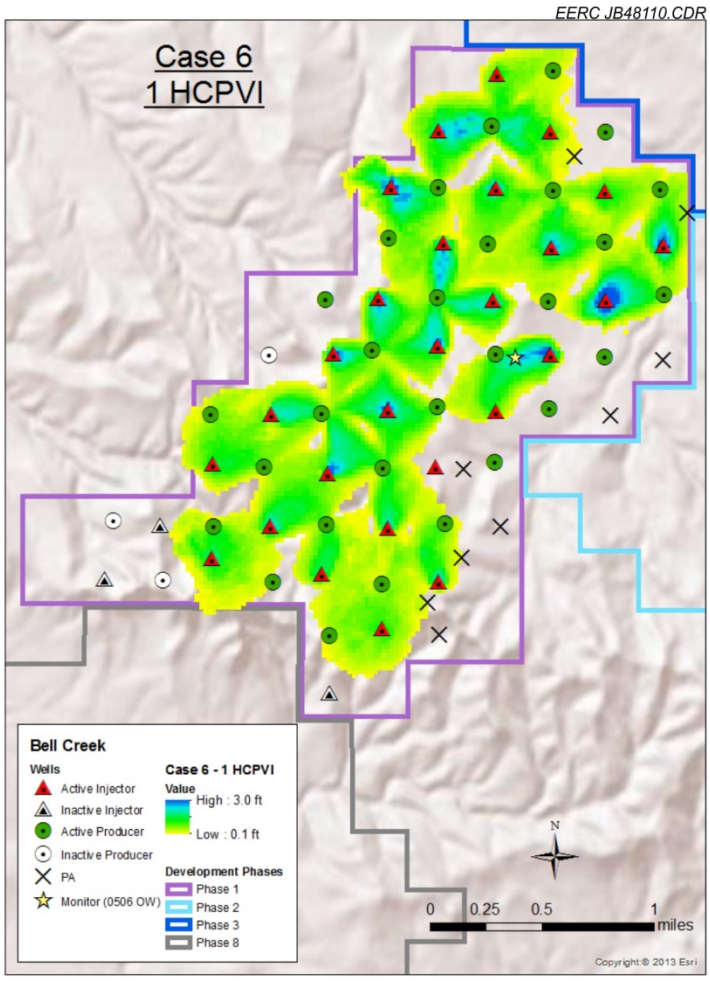

Figure 38. CO_2 plume for Case 6 (1 HCPV injected).

Future Work

This simulation study was carried out for the Phase 1 area, although the full-field geologic model had already been built. Future simulation models would include Phase 1, Phase 2, and additional phase areas.

A dynamic simulation workflow developed at the EERC will be used to conduct the sensitivity analysis, numerical tuning, and computer-aided history matching. The computer-aided history matching by CMOST will help to find the best-matched model of a reservoir. Future work also includes modeling of relative permeability hysteresis and CO_2 solubility in the aqueous phase for better estimates of CO_2 breakthrough times and storage capacity.

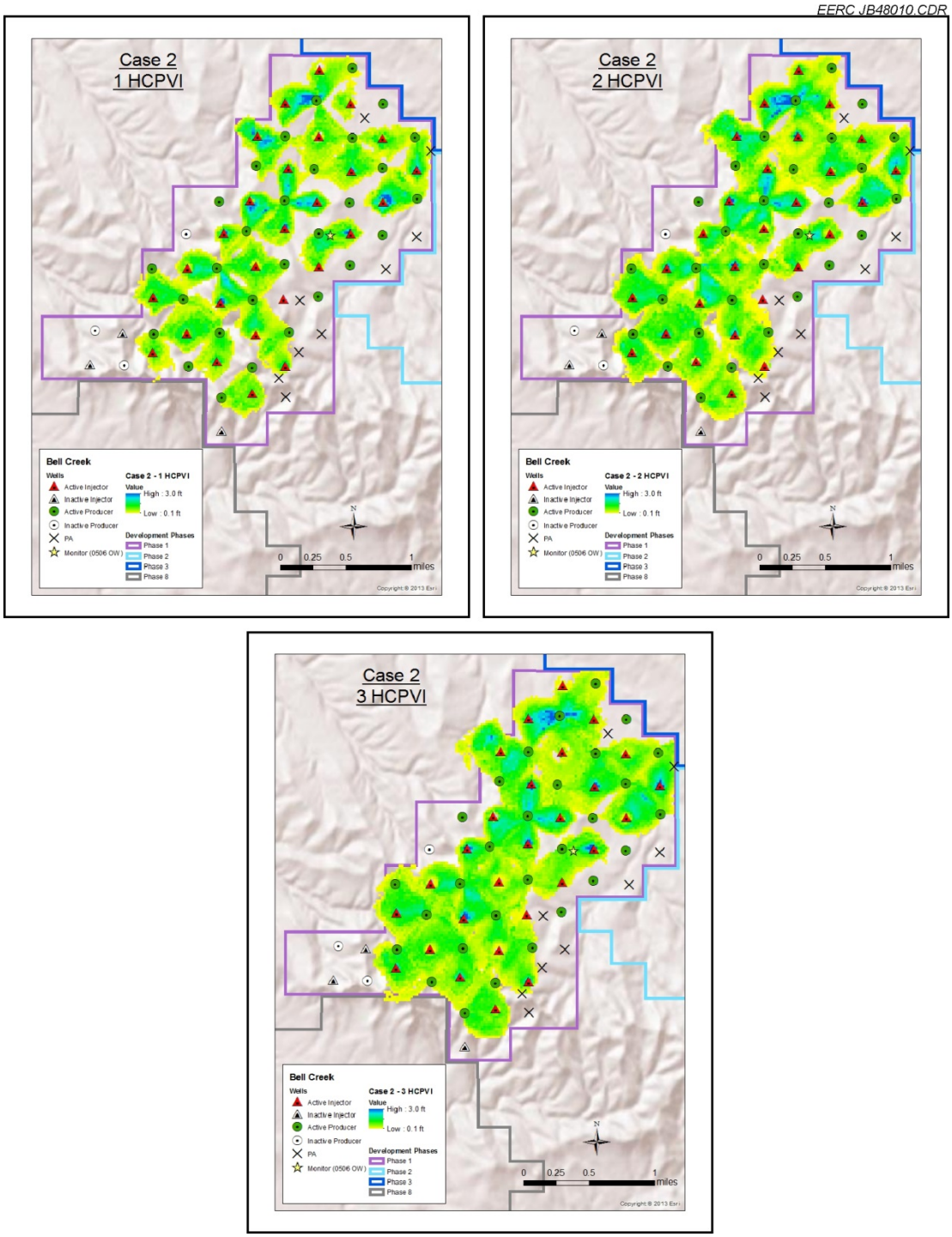

Figure 39. Case 2: areal extent of the CO_2 plume at 1, 2, and 3 HCPVI.

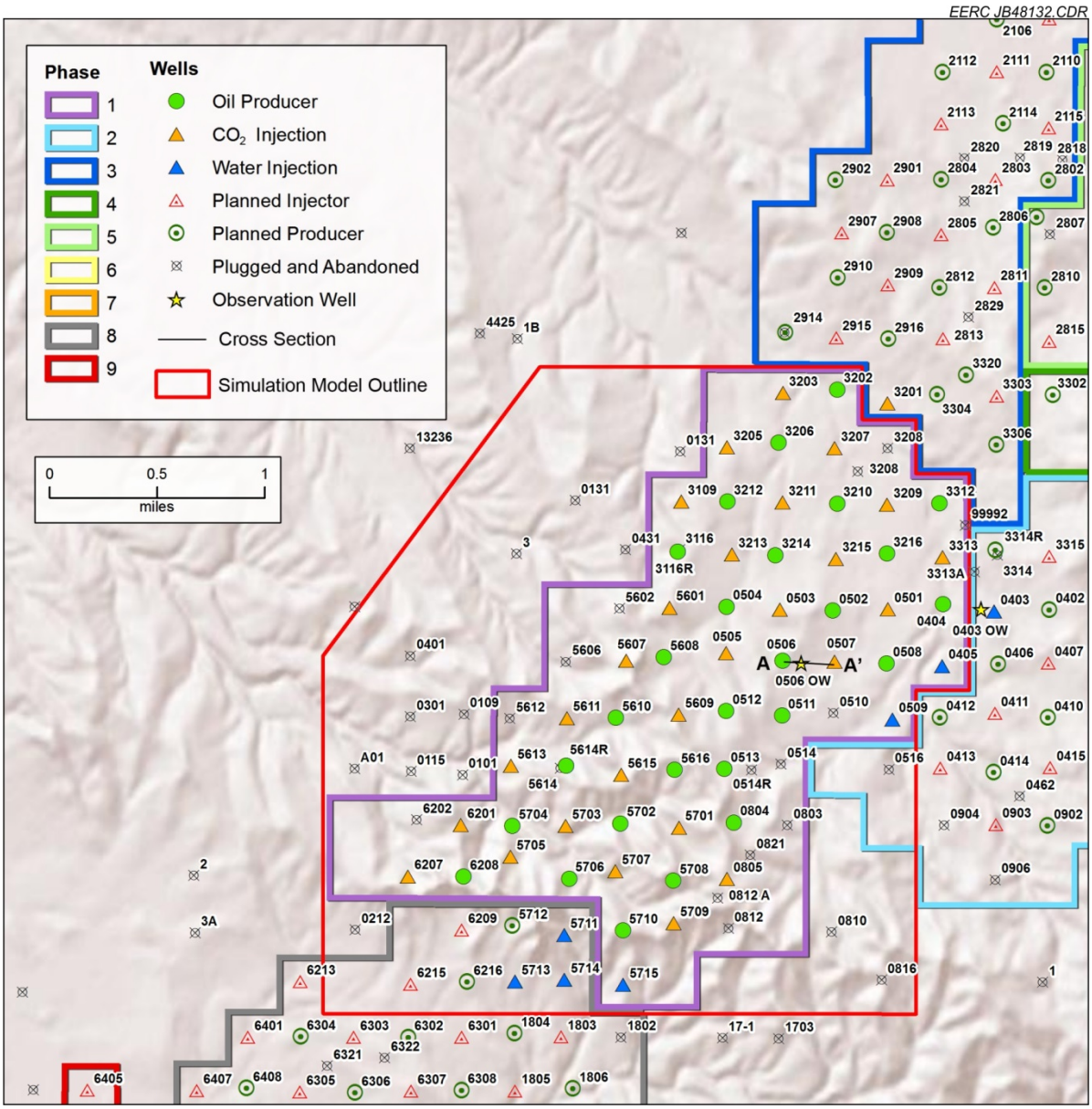

Figure 40. Map showing locations for cross section of wells 05-06, 05-06 OW, and 05-07.

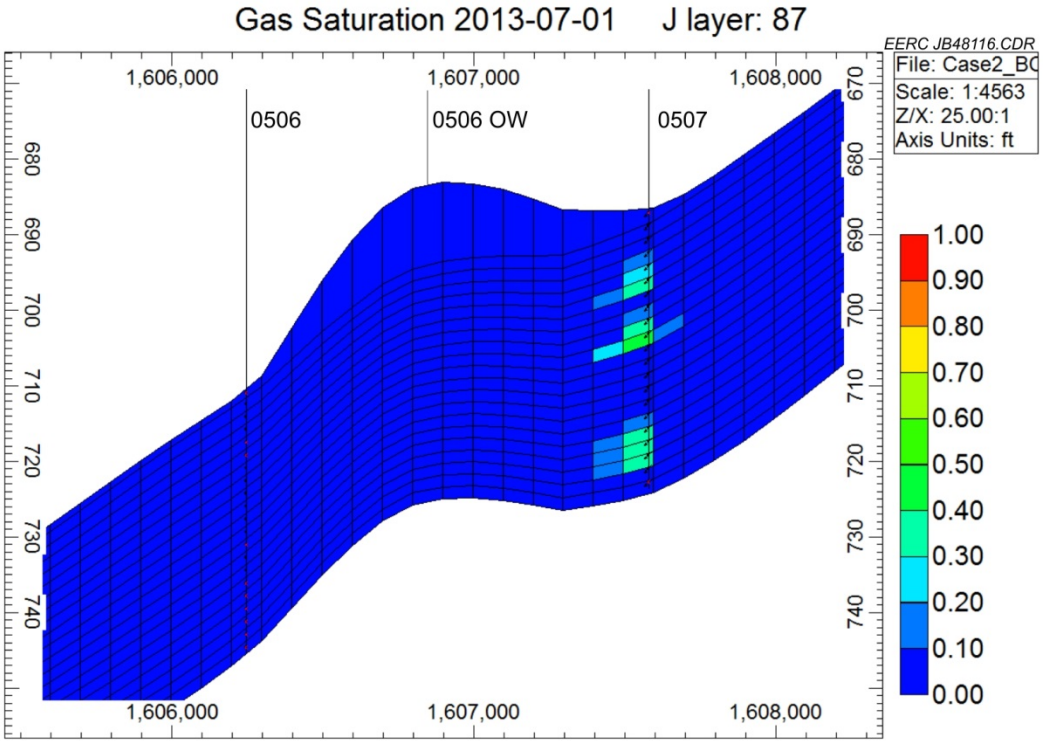

Figure 41. CO_2 saturation near the 05-06 OW monitoring well after 1 month of injection.

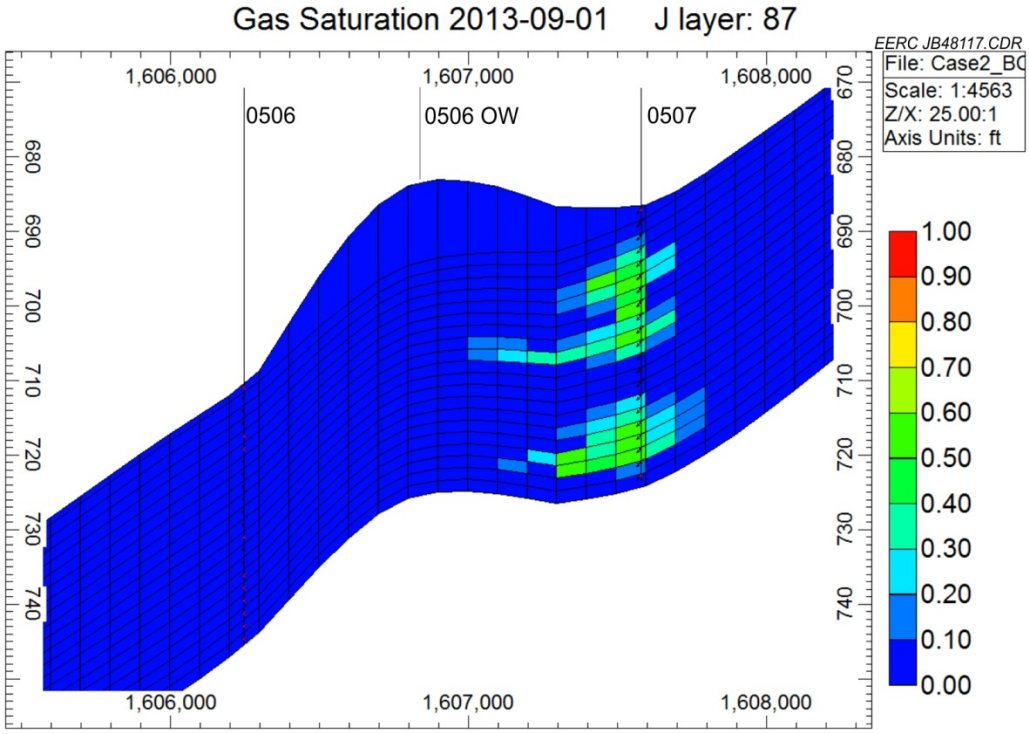

Figure 42. CO_2 saturation near the 05-06 OW monitoring well after 3 months of injection.

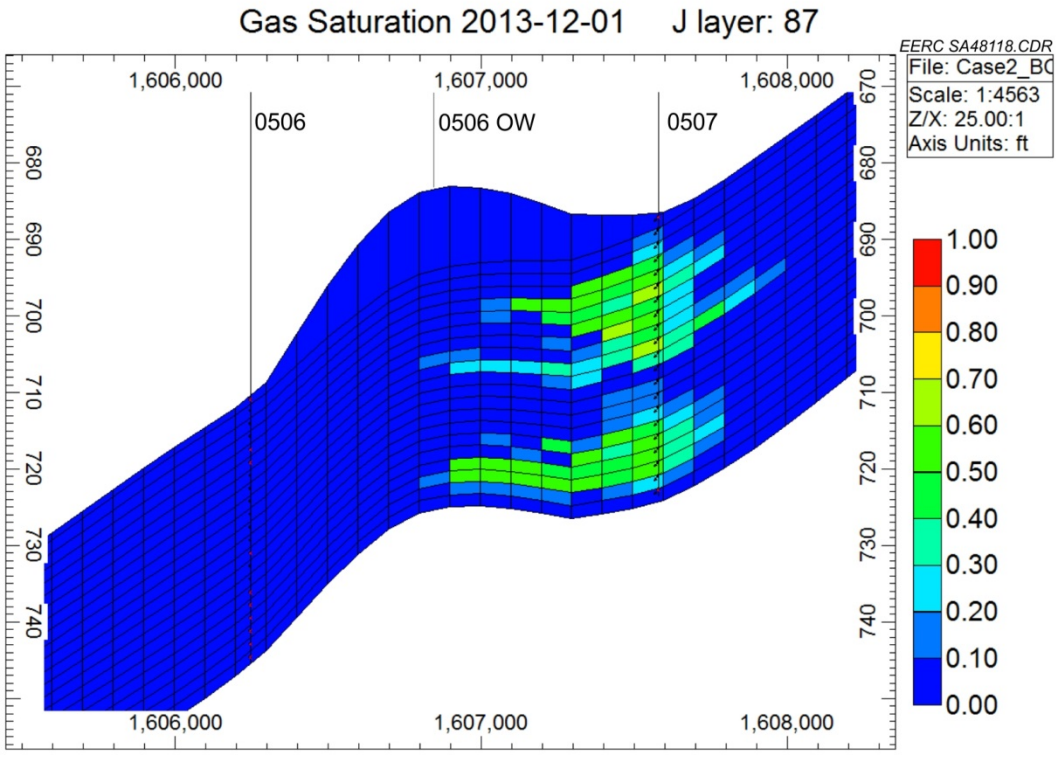

Figure 43. CO_2 saturation near the 05-06 OW monitoring well after 6 months of injection.

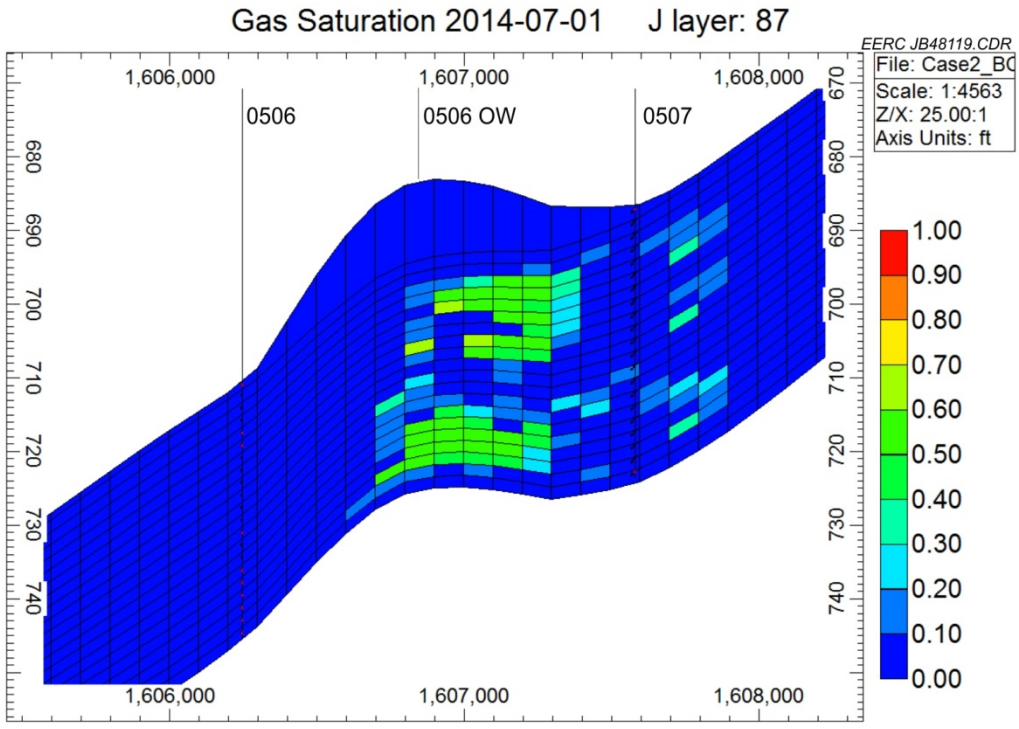

Figure 44. CO_2 saturation near the 05-06 OW monitoring well after 12 months of injection.

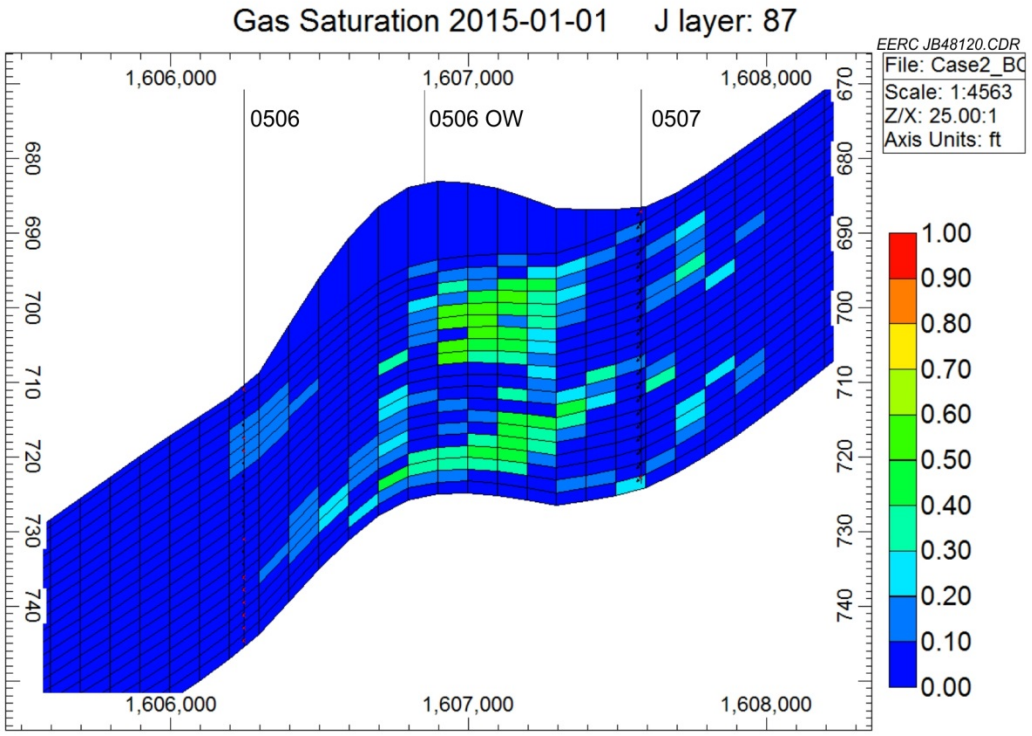

Figure 45. CO_2 saturation near the 05-06 OW monitoring well after 18 months of injection.

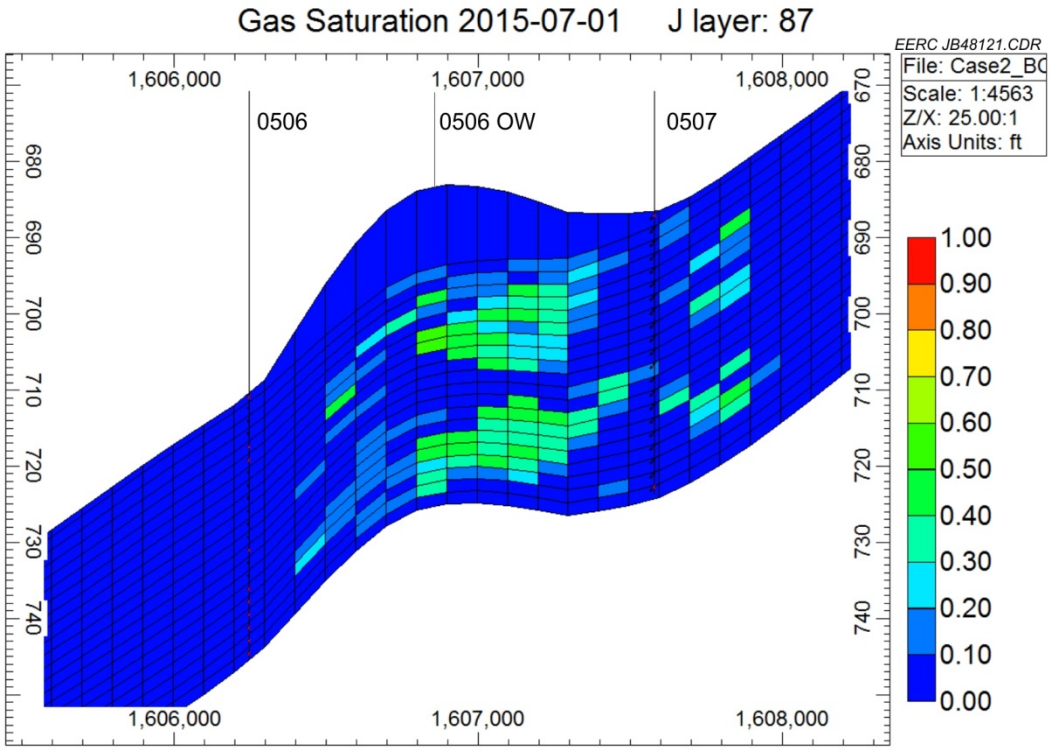

Figure 46. CO_2 saturation near the 05-06 OW monitoring well after 24 months of injection.

REFERENCES

Afsari, M., Amani, M., Razmgir, S.M., Karimi, H., and Yousefi, S., 2010, Using drilling and logging data for developing 1-D Mechanical Earth Model for a mature oil field to predict and mitigate wellbore stability challenges: www.onepetro.org/mslib/servlet/onepetropreview?id=SPE-132187-MS (accessed January 2013), SPE 132187.

Amaefule, J., and Mehmet, A., 1993, Enhanced reservoir description—using core and log data to identify hydraulic flow units and predict permeability in uncored intervals/wells: Presented at the 68th Annual Technical Conference and Exhibition, SPE 26436.

Bachman, R.C., Sen, V., and Khalmanova, D., M'Angha, V.O., and Settari, A. 2011, Examining the effects of stress dependent reservoir permeability on stimulated horizontal Montney gas wells: SPE 149331.

Computer Modelling Group Ltd., 2011, CMG's GEM user's guide: Calgary, Alberta, Computer Modelling Group, 1246 p.

Crain, E.R., 2000, Crain's petrophysical handbook: www.spec2000.net (accessed 2013).

Encore Acquisition Company, 2009, Bell Creek CO_2 project: internal report, July 2009, 8 p.

Ge, J., Klenner, R.C.L., Liu, G., Braunberger, J., Ayash, S.C., Pu, H., Gao, P., Bailey, T.P., Saini, D., Hamling, J.A., Sorensen, J.A., Gorecki, C.D., Steadman, E.N., and Harju, J.A., 2013, Bell Creek field test site – geomechanical modeling report: Plains CO_2 Reduction (PCOR) Partnership Phase III Task 9 Deliverable D32 for U.S. Department of Energy National Energy Technology Laboratory Cooperative Agreement No. DE-FC26-05NT42592, Grand Forks, North Dakota, Energy & Environmental Research Center, January.

Khan, S., Han, H., Ansari, S., and Khosravi, N., 2010, An integrated geomechanics workflow for cap rock integrity analysis of a potential carbon storage site: Presented at the International Conference on CO_2 Capture, Storage, and Utilization: New Orleans, Louisiana, November 10–12, SPE 139477.

Molnar, P.S., and Porter, M.L., 1990, Geologic reservoir study of the Bell Creek Field, Carter and Powder River Counties, Montana: Exxon USA proprietary report, Midland, Texas, 127 p.

Nagy, Z.S., Pacheco, F., Rosa, M., Riberro, M., Jouti, I., Pastor, J., Grandy, A., Fluckiger, S., and Gigena, L., 2011, Use of geomechanics for optimizing reservoir completion and stimulation strategies for carbonates in the Campos Basin, Offshore Brazil: Offshore Technology Conference: Rio De Janeiro, Brazil, October 4–6, OTC 22364.

Saini, D., Braunberger, J., Pu, H., Bailey, T.P., Ge, J., Crotty, C.M., Liu, G., Hamling, J.A., Sorensen, J.A., Gorecki, C.D., Steadman, E.N., and Harju, J.A., 2012, Bell Creek field test site – simulation report: Plains CO_2 Reduction (PCOR) Partnership Phase III Task 9 Deliverable D66 for U.S. Department of Energy National Energy Technology Laboratory Cooperative

Agreement No. DE-FC26-05NT42592, Grand Forks, North Dakota, Energy & Environmental Research Center, January.

Tao, Q., Bryant, S.L., Meckel, T.A. and Luo, Z., 2012, Wellbore leakage model for above-zone monitoring at Cranfield, MS. Carbon Management Technology Conference. Orlando, Florida, USA, 7-9 February. CMTC 151516.

Vuke, S.M., 1984, Depositional environments of the Early Cretaceous Western Interior Seaway in southwestern Montana and the northern United States, *in* Stott, D.F., and Glass, D.J., eds., The Mesozoic of Middle North America: Canadian Society of Petroleum Geologists, Memoir 9, p. 127–144.

Weimer, R.J., Emme, J.J., Farmer, C.L., Anna, L.O., Davis, T.L., and Kidney, R.L., 1982, Tectonic influence on sedimentation, Early Cretaceous, east flank Powder River Basin, Wyoming and South Dakota: Colorado School of Mines Quarterly, v. 77, no. 4.

Wulf, G.R., 1962, Lower Cretaceous Albian rocks in northern Great Plains: American Association of Petroleum Geologists Bulletin, v. 46, no. 8, p. 1372–1415.

Young, R.G., 1970, Lower Cretaceous of Wyoming and the southern Rockies: Mountain Geologist, v. 7, p. 105–121.